UC Irvine

UC Irvine Previously Published Works

Title

Upregulation of Multiple CD8+ T Cell Exhaustion Pathways Is Associated with Recurrent Ocular Herpes Simplex Virus Type 1 Infection.

Permalink

https://escholarship.org/uc/item/7108t8g1

Journal

The Journal of Immunology, 205(2)

ISSN

0022-1767

Authors

Coulon, Pierre-Grégoire
Roy, Soumyabrata
Prakash, Swayam
et al.

Publication Date

2020-07-15

DOI

10.4049/jimmunol.2000131

Peer reviewed

eScholarship.org Powered by the California Digital Library
University of California

Author Manuscript

Author Manuscript

Author Manuscript

Author Manuscript

HHS Public Access

Author manuscript

J Immunol. Author manuscript; available in PMC 2021 July 15.

Published in final edited form as:

J Immunol. 2020 July 15; 205(2): 454–468. doi:10.4049/jimmunol.2000131.

Up-Regulation of Multiple CD8+ T Cell Exhaustion Pathways is Associated to Recurrent Ocular Herpes Simplex Virus Type 1 Infection

Pierre-Grégoire Coulon[1], **Soumyabrata Roy**[#,1], **Swayam Prakash**[#,1], **Ruchi Srivastava**[1], **Nisha Dhanushkodi**[1], **Stephanie Salazar**[1], **Cassandra Amezquita**[1], **Lan Nguyen**[1], **Hawa Vahed**[1], **Angela M. Nguyen**[1], **Wasay R. Warsi**[1], **Caitlin Ye**[1], **Edgar A. Carlos-Cruz**[1], **Uyen T. Mai**[1], **Lbachir BenMohamed**[1,2,3,‡]

[1]Laboratory of Cellular and Molecular Immunology, Gavin Herbert Eye Institute, University of California Irvine, School of Medicine, Irvine, CA 92697;

[2]Department of Molecular Biology & Biochemistry; University of California Irvine, School of Medicine, Irvine, CA 92697, USA.

[3]Institute for Immunology; University of California Irvine, School of Medicine, Irvine, CA 92697, USA.

Abstract

A large proportion of the world's population harbors latent herpes simplex virus type 1 (HSV-1). Crosstalk between antiviral CD8$^+$ T cells and HSV-1 appear to control latency/reactivation cycles. We found that, compared to healthy asymptomatic (ASYMP) individuals, in symptomatic (SYMP) patients the CD8$^+$ T cells with the same HLA-A*0201-restricted HSV-1 epitope-specificities expressed multiple genes and proteins associated to major T cell exhaustion pathways and were dysfunctional. Blockade of immune checkpoints with αLAG-3 and αPD-1 antagonist mAbs synergistically restored the frequency and function of antiviral CD8$^+$ T cells, both (*i*) *ex vivo*, in SYMP individuals and SYMP HLA-A*0201 transgenic mice; and (*ii*) *in vivo* in HSV-1 infected SYMP HLA-A*0201 transgenic mice. This was associated with a significant reduction in virus reactivation and recurrent ocular herpetic disease. These findings confirm antiviral CD8$^+$ T cell exhaustion during symptomatic herpes infection and pave the way to targeting immune checkpoints to combat recurrent ocular herpes.

Keywords

Herpes simplex type 1; CD8$^+$ T cells; LAG-3; PD-1; TIGIT; TIM-3; immune checkpoint; exhaustion; blockade

‡Corresponding author: Laboratory of Cellular and Molecular Immunology, Gavin Herbert Institute; Hewitt Hall, Room 232; 843 Health Sciences Rd; Irvine, CA 92697-4390; Phone: 949-824-8937; Fax: 949-824-9626; Lbenmoha@uci.edu.

#S.R. and S.P. contributed equally to this article.

Conflict of interest: The authors have declared that no conflict of interest exists.

Author Manuscript Author Manuscript Author Manuscript Author Manuscript

INTRODUCTION

According to the most recent WHO report, more than 3.7 billion people, under the age of 50 worldwide, are currently infected with the herpes virus type 1 (HSV-1) (1). In the United States alone, ~65% adults are seropositive for HSV-1, while its prevalence in the developing world surpasses 90%, making this virus among one of the most predominant and successful human pathogens (2).

HSV-1 is usually acquired through contacts with muco-cutaneous tissues (lips, eyes, sexual mucosa and skin), where it causes a short acute infection (3). As the result of an effective primary immune responses which suppress the virus replication, the acute infection clears within days in most immunocompetent individuals (4). During the acute phase, HSV-1 gains access to the axons of the sensory neurons and travels up to gain the neuronal cell bodies in the trigeminal ganglion (TG) where it establishes lifelong latency (5–8). However, psychological, chemical and environmental stressors can trigger viral reactivation from latently-infected neurons (9). This is followed by anterograde transportation through the axons to nerve termini, shedding and re-infection of the peripheral mucocutaneous tissues. While the majority of HSV-1-infected individuals remain asymptomatic (ASYMP) even after multiple and sporadic virus reactivations from latency, a minority of symptomatic (SYMP) patients often manifest severe and repetitive recurrent herpetic diseases, sometimes multiple times a year (10, 11). In the worst case scenario, when the virus reactivates and sheds in the tears of SYMP patients, potentially blinding recurrent herpes stromal keratitis (HSK) can occur (12, 13).

Currently, an effective herpes simplex vaccine or immunotherapy is unavailable (14). Therapeutic efforts have primarily focused on restricting inflammatory disease while blocking viral replication with drugs (15–18). Antiviral $CD8^+$ T cells retained in the infected TG (19, 20) appeared to interact with infected neurons to prevent viral reactivation (21, 22). Hence, a dynamic cross-talk between functional TG-resident $CD8^+$ T cells and the virus within the latently-infected TG restrain virus reactivation (6, 23–25). However, the virus can still manage to reactivate even in the presence of an often sizable pool of virus-specific $CD8^+$ T cells in the TG, by yet-to-be determined mechanisms (7, 20, 26–28). In the present study, based on these observations and driven by our recent research using the mouse model of UV-B induced recurrent ocular herpes (20, 27), we hypothesized that: (1) repetitive reactivations of HSV-1 from latently infected TG in SYMP patients with a history of numerous episodes of recurrent corneal herpetic disease, likely induces phenotypic and functional exhaustion of the local HSV-specific $CD8^+$ T cells; and (2) Blockade of exhaustion pathways in symptomatic hosts would restore the protective efficacy of antiviral $CD8^+$ T cells, reducing virus reactivation from latently infected TG and recurrent ocular herpetic disease.

In the present study, we compared the transcriptome, phenotype, and function of memory $CD8^+$ T cells, sharing the same HLA-A*0201-restricted HSV-1 epitope-specificities freshly isolated from peripheral blood and trigeminal ganglia (TG) of HSV-1 infected ASYMP and SYMP patients and HLA transgenic (Tg) mice, respectively. We report that HSV-specific $CD8^+$ T cells from SYMP patients are phenotypically and functionally exhausted, highly co-

Author Manuscript Author Manuscript Author Manuscript Author Manuscript

expressing LAG-3 with three others inhibitory receptors (PD-1, TIGIT and TIM-3) while being defective in expression of functional markers such as, IFN-γ, Ki-67 and $CD107^{a/b}$. Moreover, the blocking of LAG-3 and PD-1 synergistically restored anti-viral $CD8^+$ T cell responses, reduced HSV-1 reactivation from latently-infected TG, and reduced UV-B induced recurrent ocular herpetic infection and disease in latently-infected HLA-A*0201 transgenic mice. These findings pave the way for a new direction using antagonist mAbs in the immune checkpoints blockade as an immunotherapeutic strategy to combat symptomatic herpes.

MATERIALS AND METHODS

Human study population and HLA-A*02:01 typing.

All clinical investigations performed in this study were conducted according to the Declaration of Helsinki. Subjects were enrolled at the University of California, Irvine, under Institutional Review Board-approved protocols (IRB#2009–6963). Written informed consent was received from all participants prior to inclusion in the study. Selected individuals screened for HSV-1 seropositivity were divided into SYMP and ASYMP groups based on the inclusion criteria, as described previously (2, 10, 29). Briefly, ASYMP individuals, despite being infected, never had any clinically-detectable recurrent herpes disease, whereas SYMP individuals reported a history of numerous episodes of clinically-documented recurrent ocular herpes diseases with one or more episodes per year for the past 5 years. Amongst the large cohort of SYMP and ASYMP individuals, 30 HLA-A*02:01-positive patients, HSV-1 seropositive – HSV-2 seronegative, were enrolled in this study (15 ASYMP and 15 SYMP; Table 1) – not to mention the patients already enrolled in the NanoString cohort (see the corresponding section below and (29)). All the individuals included were HIV- and HBV-negative with no history of immunodeficiency. SYMP and ASYMP groups were matched for age, gender, serological status, and race. Only SYMP patients who were not on Acyclovir nor on other antiviral or anti-inflammatory drug treatments and other immunosuppressive drugs at the time of blood draw were included. Pregnant or breastfeeding individuals were also excluded. Age- and sex-matched HLA-A*02:01-positive and HSV-1- and HSV-2-seronegative healthy (NEG) subjects were enrolled as controls. The HLA status of each tested individual was first screened at a two-digit level by HLA-A2 flow staining (mAbs clone BB7.2; BD Pharmingen, Inc., San Diego, CA) and the four digits HLA-A*02:01 subtype was subsequently screened by PCR on blood samples from the subjects using the PCR protocol described by Gatz S.A. et al. (30) (sense primer 5’-CCTCGTCCCCAGGCTCT and anti-sense 5’-TGGCCCCTGGTACCCGT). Cells were acquired using FORTESA flow cytometer (Becton Dickinson, Franklin Lakes, NJ). Results were analyzed with FlowJo software (BD Biosciences, San Jose, CA).

HSV-specific serotyping.

We collected sera from the donors to be tested for anti-HSV-1 and HSV-2 antibodies. Enzyme-linked immunosorbent assay (ELISA) was performed using the HerpeSelect 1 (cat. EL0920G) and HerpeSelect 2 ELISA IgG (cat. EL0910G) kits following the manufacturer’s protocol. Only individuals screened for HSV-1 seropositivity, but not HSV-2, were included in this study.

Author Manuscript Author Manuscript Author Manuscript Author Manuscript

Human peripheral blood mononuclear cells (PBMCs) isolation.

For each participant in the study, ~200 ml of blood was drawn and sera were isolated and stored at −80°C for the detection of anti-HSV-1 by ELISA, as described above. PBMCs were isolated by gradient centrifugation using leukocyte separation medium (FICOL, Life Sciences, Tewksbury, MA). The cells were resuspended in complete culture medium consisting of RPMI1640, 10% FBS (Bio-Products, Woodland, CA) supplemented with 1x penicillin/streptomycin/L-glutamine, 1x sodium pyruvate, 1x non-essential amino acids and HEPES (Life Technologies, Rockville, MD).

Cell sorting of HSV-1 specific human $CD8^+$ T cell.

HSV-specific $CD8^+$ T cells were detected using four different human tetramers, each of them specifically directed against one of the following immunodominant epitopes: (*i*) $UL43_{302–310}$ (from the envelope), (*ii*) $UL44_{400–408}$ (from the glycoprotein C), (*iii*) $gB_{561–567}$ (from the glycoprotein B), and (*iv*) $VP11/12_{220–228}$ (from the VP11/12 tegument protein). Briefly, PBMCs from either SYMP or ASYMP individuals were first incubated at 37°C for 1 hour with one of the four different PE-labeled A2-restricted HSV-specific tetramers (NIH Tetramer facility), complexed with their corresponding peptide. After washing with PBS, cells were stained with αCD3 A700 (clone HIT3a; Bio Legend) and αCD8 FITC (Cat. 555634; BD Pharmingen) antibodies in 1x PBS containing 1% FBS and 0.1% sodium azide (fluorescence-activated cell sorting [FACS] buffer) for 1 hour at 4°C. Following the addition of 7AAD (Cat. 51–68981E; BD Pharmingen – 3 μl/10^6 cells) into the samples for exclusion of apoptotic and dead cells, the sorting of the HSV-specific $CD8^+$ T cells was performed using a FACS Aria II (BD Biosciences).

Bulk RNASeq on sorted $VP11/12_{220–228}$-HSV-specific $CD8^+$ T cells.

RNA was isolated from the sorted $VP11/12_{220–228}$-specific $CD8^+$ T cells using the Direct-zol RNS MiniPrep (Zymo Research, Irvine, CA) according to the manufacturer's instructions. RNA concentration and integrity were determined using the Agilent 2100 Bioanalyzer. Sequencing libraries were constructed using TruSeq Stranded Total RNA® Sample Preparation Kit (Illumina, San Diego, CA). Briefly, rRNA were first depleted using the Ribo-Gone rRNA removal kit (Clonetech, Mountain View, CA) before the RNA was fragmented, converted to ds cDNA and ligated to adapters, amplified by PCR and selected by size exclusion. Following quality control for size, quality, and concentrations, libraries were multiplexed and sequenced to single-end 100 bp sequencing using the Illumina HiSeq 4000 platform.

Differentially-expressed genes (DEGs) were analyzed by using integrated Differential Expression and Pathway analysis (iDEP) tools. iDEP seamlessly connects 63 R/Bioconductor packages, 2 web services, and comprehensive annotation and pathway databases for multiple animal species including that of human and rabbit. Expression matrix of DEGs was filtered and converted to Ensemble gene IDs, and the pre-processed data was used for exploratory data analysis (EDA) including k-means clustering and hierarchical clustering. The pairwise comparison of human (ASYMP vs. SYMP) was performed using the DESeq2 package with a threshold of false discovery rate (FDR) < 0.5. and fold-change >

Author Manuscript Author Manuscript Author Manuscript Author Manuscript

1.5. For the construction of the heat map, T cells exhaustion-related genes were selected on the basis of the curated GSEA gene list GSEA9650_1257_200_UP (31).

NanoString assay on various sorted HSV-specific CD8$^+$ T cells.

The NanoString assay used in this study and its corresponding cohort of HLA-A*02:01-positive, HSV-seropositive symptomatic and asymptomatic individuals, has been previously described by our laboratory (29). We used a commercially-available human gene panel, nCounter Immunology v2 (human), containing 579 unique human genes (29) known to be broadly relevant in the immune responses, including 15 housekeeping genes and six positive controls (NanoString Technologies, Seattle, WA). RNA was isolated from either $UL43_{302–310}$-, $UL44_{400–408}$-, $gB_{561–567}$-, or $VP11/12_{220–228}$-specific CD8$^+$ sorted T cells coming from 10 ASYMP or 10 SYMP individuals, using the Direct-zol RNS MiniPrep (Zymo Research) according to the manufacturer's instructions. Reporter and capture probes were hybridized during a 20 hours incubation at 65°C, and the resulting RNA complexes were subsequently immobilized and counted on an nCounter analyzer (NanoString Technologies) according to the manufacturer's instructions. Raw data were normalized in nSolver 3.0 based on the geometric mean of negative controls, internal housekeeping genes, and positive controls. Normalized counts from genes included in the immune panels and fulfilling the minimum count requirement were averaged before additional analysis.

Human T cell flow cytometry: surface & tetramer staining followed by intracellular staining for functional assay.

PBMCs from each individual were stained for cell-line phenotypic markers, HSV-1 specific HLA-A*02:01 restricted tetramers, surface exhaustion immune checkpoint receptors and (when needed) intracellular functional cytokines (Intracellular Cytokines Staining – ICS). To analyze the phenotype and the frequency of the HSV-specific CD8$^+$ T cells recognizing VP11/12 peptide/HLA-A2 complexes, PBMCs were first incubated with $VP11/12_{220–228}$ peptide/ HLA-A2 tetramer complex for 1 hour at 37°C. Cells were alternatively stained with the EBV $BMLF\text{-}1_{280–288}$ specific tetramer (32) used as control. Cell preparations were washed twice with FACS buffer and stained 45 min. on ice, in the dark, with the following mAbs against cell-surface markers: anti- CD3 BUV395 (clone SK7; BioLegend, San Diego, CA), CD8 BV711 (clone SK1; BioLegend), CD4 BV421, PD-1 FITC (clone EH12.2H7; BioLegend), LAG-3 PerCPCy5.5 (clone 11C3C65; BioLegend), TIGIT PE/Cy7 (clone A15153G; BioLegend), TIM-3 APC/Cy7 (clone F38–2E2; BioLegend), CTLA-4 APC (clone L3D10; BioLegend), PSGL-1 A700 (clone 688101; R&D systems), GITR APC (clone 108–17; BioLegend), BTLA PE/Cy7 (clone MIH26; BioLegend) and AQUA (live/dead kit; Thermo-Scientific, Cat. L34966). After washing three times, the cells were then fixed for 20 minutes on ice using PBS 1× 2% paraformaldehyde and resuspended in 300 μl FACS buffer before acquisition. All staining was performed in duplicate. For each sample, a total of 5×10^6 cells were stained, and 100,000 CD3$^+$ cells-events (approximately 150,000 to 350,000 lymphocyte gated cells) were acquired on the BD FORTESA.

To measure the functionality of the CD8$^+$ T cells specific for $VP11/12_{220–228}$ (or $gB_{561–567}$, $UL43_{302–310}$ and $UL44_{400–408}$) we also performed an intracellular assay (ICS) to detect IFN-γ and Ki-67, combined with a $CD107^{a/b}$ staining. 5×10^6 PBMCs in a 96-well plate

Author Manuscript Author Manuscript Author Manuscript Author Manuscript

were stimulated *in vitro* with peptide (10 μg/ml/peptide) at 37°C overnight. An additional six hours of incubation with the BD Golgi Stop / Golgi Plug (BD Biosciences), 10 μl of anti-CD107^{a} A647 (clone H4A3; BD Biosciences) and of anti-CD107^{b} A647 (clone H4B4; BD Biosciences) was performed before the cells were washed twice with FACS buffer. We then proceeded to the tetramer and the surface staining as previously mentioned. After surface staining, the cells were fixed using BD Cytofix/Cytoperm permeabilization and fixation solution for 20 minutes at 4°C. Intracellular staining then started by adding the following antibodies: IFN-γ A700 (clone B27, BD Pharmingen), Ki-67 PE-Cy7 (clone 20Raj1; Invitrogen, Carlsbad, CA) – for 45 min. on ice in 1x PermWash Buffer (BD), followed by three washes with the same buffer. Finally, cells were resuspended in 300 μl FACS buffer before acquisition.

Along with the single-color stained PBMCs, Ab capture beads (BD Biosciences) were used as individual compensation tubes for each fluorophore. To define positive and negative populations, we used fluorescence minus controls for each fluorophore along with isotype control mAbs and we further optimized gating by examining known negative cell populations for background expression levels. Briefly (as described in Fig. S1), we gated on the lymphocyte population, single cells, viable cells (Aqua Blue^{-}), CD3^{+} cells, and CD8^{+} cells before finally gating on tetramers-positive HSV-specific CD8^{+} T cells. Data analysis was performed using FlowJo 10 software (BD Bioscience).

PD-1 and LAG-3 in vitro blockade on human PBMCs.

ASYMP and SYMP PBMCs were collected, seeded in a 96-well plate (1×10^{6} cells per well) and stimulated with 10 μg/ml of the VP11/12$_{220–228}$ peptide. Twenty-four hours after peptide stimulation, anti-human PD-1 mAb (clone J110 from BioXcell – West Lebanon, NH), anti-human LAG-3 mAb (clone 17B4 from Enzo-Life Sciences described here (33)) or a combination of both were added to the culture at 10 μg/ml for 2 more days with the culture medium being replenished every day with the addition of fresh peptide and blocking antibodies at the same concentrations. Cells were then stained and measured for the expression of surface exhaustion markers as well as the production of functional cytokines by the VP11/12$_{220–228}$ specific CD8^{+} T cells.

HSV-1 viral production and ocular infection of HLA-A2 transgenic mice.

Animal studies were conducted with the approval of the Institutional Animal Care and Use Committee (IACUC) of University of California-Irvine (Irvine, CA) and conformed to the Guide for the Care and Use of Laboratory Animals published by the US National Institute of Health (IACUC protocol #FG19402). HLA-A*02:01 transgenic (Tg) mice ((34, 35)) were kindly provided by Dr. Francois Lemonier (Pasteur Institute, Paris, France) and were bred at University of California Irvine. These mice represent the F1 generation resulting from a cross between HLA-A*02:01/Kb Tg mice (expressing a chimeric gene consisting of the 1 and 2 domains of HLA-A*02:01 and the 3 domains of H-2Kb) created on the BALB/c genetic background. Eight weeks-old mice with an equivalent male/female ratio were used for this study.

Author Manuscript Author Manuscript Author Manuscript Author Manuscript

The HSV-1 (strain McKrae) was propagated in RS cells as described previously (36) and the virus was subsequently purified by ultracentrifugation in sucrose gradient and titrated via the plaque assay. All mice were ocularly infected with 2×10^5 PFU of strain McKrae via eye drops (3 μL) after corneal scarification (i.e. light crosshatched pattern of 4 vertical and 4 horizontal scratches using a 25-gauge needle).

PD-1 and LAG-3 blockade on mouse DLN lymphoid cells and trigeminal ganglion explants.

HLA-$A2^+$ Tg mice (n=10) were ocularly infected for 14 days as described above. Both the submandibular draining lymph node (DLN) and trigeminal ganglion (TG) were individually harvested.

DLN homogenates were prepared by pressing the tissues through a sterile mesh screen into 5 ml of PBS 1x under aseptic conditions. Subsequently, they were resuspended in supplemented RPMI 1640 medium + 10% FBS to obtain single-cell suspensions. Cells were then plated in 96-well plates (2×10^6 cells per well) and stimulated overnight with 10 μg/ml of the HSV-1 $VP11/12_{220–228}$ peptide before anti-mLAG-3, anti-mPD-1 (clone J43; BioXcell West Lebanon, NH), blocking antibodies were added in the culture for two more days, at two different doses (10 μg/ml or 30 μg/ml). After two days of blockade (day 3 post-stimulation), cells were first incubated with $VP11/12_{220–228}$ peptide/ HLA-A2 tetramer complex for 30–45 min. at 37°C. Cells were then washed and surface-stained for 30 minutes on ice in the dark, with mAbs against mouse CD8 BUV395 (clone 53–6.7; BD Horizon), CD4 BV510 (clone RM4–5; BioLegend), CD3 BV421 (clone 17A2; BioLegend), LAG-3 PercP/Cy5.5 (clone C9B7W; BioLegend) and PD-1 APC (clone 29F.1A12; BioLegend). The intracellular assay to detect IFN-γ, $CD107^{a/b}$ and Ki-67 was performed as aforementioned in humans, using anti-mouse anti-IFN-γ A700, (clone XMG1.2; BioLegend), anti-$CD107^{a/b}$ FITC (clones 1D4B and M3/84; BD Pharmingen) and anti-Ki-67 PE-Cy7 (clone 16A8; BioLegend).

The TG from infected HLA-$A2^+$ mice were excised, pooled and finely chopped and placed into culture with RPMI 1640 medium + 2 % FBS. Cultures in duplicates were then incubated at 37°C for 10 days with 100 μg/ml of blocking mAbs, targeting mPD-1 (clone J43; BioXcell), mPD-L1 (clone 10F.9G2; BioXcell), mLAG-3 (clone C9B7W; BioXcell), mIFN-γ (clone XMG1.2; BioXcell), mIFN-γR (clone GR-20; BioXcell), and mCD8 (clone 116–13.1 HB129; BioXcell). On alternate days until day 10 post explant (days 2, 4, 6, 8), the mAbs were replenished and 600 μl of culture supernatant fluid was removed from each culture, stored at −80°C for the virus titration, and replaced with an equal volume of fresh medium.

The supernatant from TG was assayed for infectious HSV-1 by plaque assay, as previously described ((12)). Briefly, 300 μl from each supernatant sample were placed on top of RS cells (90% confluent) plated in 12-well plates on a rocking machine at room temperature for two hours. Next, the supernatants were removed and replaced with medium containing carboxy-methyl cellulose. After 48 hours of incubation at 37°C, cells were fixed, stained with crystal violet and viral plaques were counted.

Author Manuscript Author Manuscript Author Manuscript Author Manuscript

UV-B induced reactivation of HSV-1 from latency in mice.

Thirty-five days post-infection, when latency was fully established, reactivation of latent HSV-1 infection was induced by UV-B irradiation in all groups of mice ((8)). TM20 Chromato-Vu transilluminator (UVP, San Gabriel, CA), which emits UV-B at a peak wavelength of 302 nm was used for this purpose. Anesthetized (Intraperitoneal (IP) injection of ketamine/xylazine mouse cocktail 0.1 mL/20g mouse containing 87.5 mg/kg ketamine and 12.5 mg/kg xylazine) mice were placed on the transilluminator, and each mouse was positioned on a piece of cardboard containing a hole the same size as the mouse's eye allowing just the eyes to be irradiated with 250 mJ/cm^2 of UV-B light (60-s exposure on the transilluminator).

Monitoring of ocular herpes infection and disease in latently infected mice.

Following ocular infection and UV-B reactivation, mice were monitored for ocular herpes virus infection and disease. Virus shedding after reactivation by UV-B irradiation was quantified in eye swabs collected every day up to day 8 post-UV-B. Eyes were swabbed using moist type 1 calcium alginate swabs and frozen at −80 °C until titrated on RS cell monolayers, as described previously ((37, 38)). Animals were examined for signs of recurrent corneal herpetic disease by slit lamp for 30 days post UV-B radiation by investigators who were blinded to the treatment regimen of the mice and scored according to a standard 0 – 4 scale (0 = no disease; 1 = 25%; 2 = 50%; 3 = 75%; 4 = 100%) as previously described ((39)). Total disease score of each day in each group of mice till 30 days post-UV-B exposure was noted. Cumulative graphs of eye disease were generated by dividing the total score of each day per group of mice by the total number of eyes in each group and adding the value to that obtained in the succeeding day and continuing until day 30 post-UV-B. Similarly, cumulative graphs of the number of eyes showing recurrent keratitis were done by dividing the total number of eyes showing disease per group of mice (irrespective of disease severity) by the total number of eyes in each group and adding the value to that obtained in the following day and continuing till 30-days post-UV-B. The average of the total score of each group for each of the 30 days post UV-B was calculated by dividing the total score of each day by the total number of eyes in each group.

PD-1 and LAG-3 in vivo blockade in latently infected mice.

The same blocking antibodies against PD-1 and LAG-3 from BioXcell used on TG explant *ex vivo*, were used here for the reactivation studies. Briefly, latently infected mice were exposed to UV-B irradiation on day 35 post-infection, and subsequently received intraperitoneal (I.P.) injections of α-PD-1 mAb and/or α-LAG-3 mAbs (200 μg/dose), on day 37, 39 and 41 post-infection.

Isolation of cornea- and TG-resident leukocytes in latently infected mice for flow cytometry staining.

Mice from all groups were euthanized, and the cornea and TG were individually harvested. Cornea and TG tissues were digested in complete medium containing 2.5-mg/ml collagenase type IV (Sigma Chemical Co., St. Louis, MO). Digestion was accomplished by incubation at 37°C with shaking for 30 minutes. After digestion, tissues and cells were filtered through a

Author Manuscript Author Manuscript Author Manuscript Author Manuscript

sterile gauze mesh and washed with RPMI 1640 medium. Single-cell suspensions were stained with the following anti-mouse antibodies: CD3 FITC (clone17A2; Biolegend), CD8 PerCP (clone 53–6.7; BD), CD4 PE/Cy7 (clone GK1.5; Biolegend), IFN-γ-PE (clone XMG1.2; BioLegend), CD107^a FITC (clone 1D4B; BD), CD107^b FITC (clone Ha1/29; BD), and Ki-67 PE/Cy7 (clone 16A8; BioLegend). The surface and the ICS staining protocol were the same as aforementioned. Cells were acquired with the BD FORTESA cytometer.

Statistical analysis.

Data for each assay were compared by Student's *t*-test or ANOVA multiple comparison procedures using GraphPad Prism version 8 (La Jolla, CA). Data are expressed as the mean ± SD. Results were considered statistically significant at a *P* value of ≤ 0.05.

RESULTS

1. Genes associated to multiple T cell exhaustion pathways are up-regulated in HSV-specific CD8$^+$ T cells from symptomatic herpes patients:

As illustrated in Fig. 1A, we first compared: (*i*) the frequencies of HSV-specific CD8$^+$ T cells from SYMP and ASYMP individuals; and (*ii*) the immune gene signatures associated with HSV-specific CD8$^+$ T cells, that share the same HSV-1 epitope specificities, but derived from either SYMP or ASYMP individuals. There were no significant differences in the percentages nor in the numbers of HSV-1 VP11/12$_{220–228}$-specific CD8$^+$ T cells detected in PBMCs of SYMP vs. ASYMP individuals (Fig. 1B). To determine any transcriptional profiling differences, VP11/12$_{220–228}$-specific CD8$^+$ T cells were sorted from the blood of SYMP and ASYMP individuals, and total mRNA was subjected to whole transcriptome analysis using bulk RNA sequencing (Fig. 1C) and NanoString digital barcoding technology (Fig. 1D).

The RNASeq analysis revealed two different patterns of gene expression in VP11/12$_{220–228}$-specific CD8$^+$ T cells from SYMP compared to VP11/12$_{220–228}$-specific CD8$^+$ T cells from ASYMP individuals (Fig. 1C). We focused on the major differences detected in the expression of genes associated with T cell exhaustion signaling pathways (based on the GSEA resource #GSEA9650_1257_200_UP). Compared to VP11/12$_{220–228}$-specific CD8$^+$ T cells from ASYMP individuals, the VP11/12$_{220–228}$-specific CD8$^+$ T cells from SYMP patients, the bulk RNASeq displayed a significant upregulation of *PD-1, LAG-3, TIGIT, TIM-3, CTLA-4, PSGL-1* and *BTLA* genes ($P = 0.0001$, $P = 0.0004$, $P = 0.001$, $P = 0.003$, $P = 0.005$, $P = 0.0002$ and $P = 0.0003$, respectively) (Fig. 1D). This was confirmed using the NanoString digital barcoding technology (Fig. 1E). Besides the well-known exhaustion-related genes, genes for others recently described inhibitory receptors, such as the CD160, the 2B4, PRDM-1 and the prostaglandin receptor PTGER4 were also significantly upregulated in VP11/12$_{220–228}$-specific CD8$^+$ T cells from SYMP individuals (Figs. 1C). In contrast, other genes such as *Ly49b* were downregulated while *GITR* showed no change in expression in VP11/12$_{220–228}$-specific CD8$^+$ T cells from SYMP compared to ASYMP individuals (Figs. 1C and 1D). Moreover, the upregulation of exhaustion-related genes observed in VP11/12$_{220–228}$-specific CD8$^+$ T cells from SYMP individuals was confirmed in

Author Manuscript Author Manuscript Author Manuscript Author Manuscript

$CD8^+$ T cells specific against three other additional HSV-1 epitopes: $gB_{561–567}$, $UL43_{302–310}$, or $UL44_{400–408}$ (Figs. 1E). Although there were slight quantitative differences in the upregulation levels of those genes amongst SYMP $CD8^+$ T cells specific to various epitopes, the trend remained the same.

Accordingly, many functional genes were downregulated in HSV-specific $CD8^+$ T cells from SYMP patients. These included: (*i*) T cell activation and differentiation genes, *CD44* and *CD69*; (*ii*) T cell antiviral genes, *IFN-γ, CD107, IL-2, p55, TNF-R1*; (*iii*) the cytokine signaling genes, *IL-17R, IL-4R, IL-12B, IL-18R1*; and (*iv*) homeostatic and T cells self-renewal genes, *IL-7, IL-15* and their receptors. In addition, the deficiencies in cytokine signaling was not restricted to the expression of cell-surface receptors since the kinases Jak1, Jak3, and Stat5, key components of cytokine signaling pathways in T cells were also downregulated in HSV-specific T cells from SYMP individuals (Fig. 1C).

Moreover, in conformity with the GSEA resource #GSEA9650_1257_200_UP findings, genes for several transcription factors were also altered in their expression profile in HSV-specific $CD8^+$ T cells from SYMP individuals (Fig. 1C). Some transcription factors genes were upregulated (*MYC, Maf*) while others were downregulated (*Fos, FosB*). Several Klf family members were also identified as downregulated in exhausted $CD8^+$ T cells including *Klf2, Klf3 and Klf13*. In addition, the expression of *Rabac1* gene, involved in vesicle transport, was downregulated in HSV-specific $CD8^+$ T cells from SYMP individuals. In contrast, anti-inflammatory and immunoregulatory genes such as *IL-10* was upregulated in HSV-specific $CD8^+$ T cells from SYMP individuals.

These results demonstrate that while HSV-1 seropositive SYMP and ASYMP individuals displayed similar frequencies of HSV-specific $CD8^+$ T cells, a side-by-side comparison of differentially expressed immune genes (DEGs) in HSV-specific $CD8^+$ T cells from SYMP vs. ASYMP individuals sharing the same epitope specificities pointed to a significant upregulation of multiple genes associated to phenotypic and functional exhaustion in HSV-specific $CD8^+$ T cells from SYMP patients who are clinically diagnosed with severe and repetitive recurrent ocular herpetic disease.

2. PD-1, LAG-3, TIGIT and TIM-3 exhaustion receptors are up-regulated on the surface of HSV-specific $CD8^+$ T cells from symptomatic herpes patients:

We next determined whether the differential expression of the genes associated to T cell exhaustion pathways would reflect a differential expression of the exhaustion receptors on the surface of HSV-specific $CD8^+$ T cells. As illustrated in Fig. 2A, blood-derived HSV-1 $VP11/12_{220–228}$ specific $CD8^+$ T cells from SYMP and ASYMP individuals ($n = 10$) were analyzed by flow cytometry for the expression of *PD-1, LAG-3, TIGIT, TIM-3, PSGL-1, GITR, BTLA and CTLA-4*, using the gating strategy shown in Fig. S1.

Compared to ASYMP individuals, SYMP patients showed significantly higher frequencies of $VP11/12_{220–228}$ epitope-specific $CD8^+$ T cells expressing PD-1, LAG-3, TIGIT and TIM-3 exhaustion receptors ($P < 0.01$ for PD-1, LAG-3 and TIGIT and $P < 0.02$ for TIM-3) (Figs. 2B and 2C). Moreover, significantly higher expression levels of PD-1, LAG-3, TIGIT and TIM-3 were detected on the surface of $VP11/12_{220–228}$-epitope-specific $CD8^+$ T cells of

Author Manuscript Author Manuscript Author Manuscript Author Manuscript

SYMP patients compared to ASYMP healthy individuals, confirming the transcriptome results shown in Fig. 1 ($P \leq 0.05$, Fig. 2D). In contrast, there was no significant differences in the expression levels of PSGL-1, GITR, BTLA and CTLA-4 on the surface of VP11/12$_{220–228}$-epitope-specific CD8$^+$ T cells of SYMP and ASYMP individuals. Human herpes viruses are important causes of potentially severe chronic infections for which functional CD8$^+$ T cells specific for several HSV epitopes are believed to be necessary for control. Alike our observations on VP11/12$_{220–228}$ epitope-specific CD8$^+$ T cells in SYMP individuals, we showed a similar exhaustion profile of CD8$^+$ T cells specific to three others HSV-1 epitopes (gB$_{561–567}$, UL43$_{302–310}$ or UL44$_{400–408}$), with an upregulation of LAG-3 and PD-1 in SYMP individuals only (Fig. S2A and 2B). In contrast, EBV (BMLF-1$_{280–288}$) and CMV (pp65$_{595–603}$) -specific CD8$^+$ T cells derived from the same SYMP individuals were functional, suggesting that the exhaustion was specific to HSV-1 epitopes (Fig. S2).

Altogether, these results confirm that the major exhaustion pathways, PD-1, LAG-3, TIGIT and TIM-3, are highly up-regulated in the HSV-specific CD8$^+$ T cells from SYMP patients.

3. Multiple exhaustion receptors are co-expressed on the surface of dysfunctional HSV-specific CD8$^+$ T cells detected from symptomatic herpes patients:

The co-expression of PD-1, LAG-3, TIGIT and TIM-3 exhaustion receptors was determined on the surface of HSV-1 VP11/12$_{220–228}$-specific CD8$^+$ T cells from SYMP vs. ASYMP individuals. PD-1, TIGIT and TIM-3 were found to be expressed together with LAG-3 on the surface of 24.8%, 48.2% and 17% of VP11/12$_{220–228}$-specific CD8$^+$ T cells from SYMP patients, respectively (Fig. 3A, *upper row*). In contrast, only 2.6%, 12.9% and 8.7% of VP11/12$_{220–228}$-specific CD8$^+$ T cells from ASYMP individuals co-expressed those markers, respectively (Fig. 3A, *upper row*). Those differences were significant not only at the percentage levels ($P \leq 0.0005$), but also in absolute numbers ($P \leq 0.01$) (Fig. 3B, *left panels*).

The co-expression patterns of multiple exhaustion receptors were specific to HSV-1 CD8$^+$ T cells. In the same SYMP and ASYMP individuals, in contrast to HSV-1 VP11/12$_{220–228}$-specific CD8$^+$ T cells, the frequencies of CD8$^+$ T cells specific to an irrelevant HLA-A*02:01-restricted EBV epitope (BMLF-1$_{280–288}$ (32)) co-expressing LAG-3 together with PD-1, with TIGIT or with TIM-3 were comparatively low (~3–10%, ~5–10% and ~8–12%, respectively) (Fig. 3A *–lower row* and Fig. 3B *– right panel*). More importantly, there was no significant difference in the frequency and number of the BMLF-1$_{280–288}$-specific CD8$^+$ T cells co-expressing the four exhaustion markers between the SYMP and ASYMP groups (Fig. 3A *–lower row* and Fig. 3B *– right panel*).

Moreover, as evidenced in Fig. 3C, a significantly lower proportion of VP11/12$_{220–228}$-specific CD8$^+$ T cells expressing IFN-γ were detected in SYMP (~10%) as compared to ASYMP individuals (~15%) (P=0.01) and we observed the same trend in other HSV-specific CD8$^+$ T cells specific for gB$_{561–567}$, UL43$_{302–310}$ or UL44$_{400–408}$ from SYMP individuals (Fig. S2C). Similarly, a lower proportion of VP11/12$_{220–228}$-specific CD8$^+$ T cells expressing CD107$^{a/b}$ and Ki-67 were also detected from SYMP compared to ASYMP individuals (respectively ~8% vs. ~10–12% for CD107$^{a/b}$ and ~19% vs. ~27% for Ki-67) ($P \leq 0.02$, Fig. 3C). As expected, a lower frequency of HSV-specific LAG-3$^+$CD8$^+$ T cells

Author Manuscript Author Manuscript Author Manuscript Author Manuscript

produced IFN-γ (~6% of IFN-γ^+ cells) compared to higher frequency of HSV-specific LAG-3^-CD8^+ T cell counterpart (~15%) ($P < 0.0001$) (Fig. 3D). It is noteworthy to mention that the proportion of $VP11/12_{220–228}$-specific LAG-$3^+TIM\text{-}3^+CD8^+$ cells producing IFN-γ was even lower as depicted in Fig. 3D (P=0.03).

These results demonstrate a higher proportion of dysfunctional HSV-specific $CD8^+$ cells co-expressing multiple exhaustion receptors are present in SYMP individuals. Moreover, a low frequency of EBV-specific $CD8^+$ T cells were expressing PD-1, LAG-3, TIGIT or TIM-3 exhaustion markers in SYMP and ASYMP individuals. Since those cells were detected at the same proportion in both groups, with no differences in their ability to produce IFN-γ (Fig. S2C), this indicate that the observed exhaustion is restricted to HSV-specific $CD8^+$ T cells in SYMP individuals.

4. Blockade of LAG-3 and PD-1 immune checkpoints synergistically restored the frequency and function of HSV-specific $CD8^+$ T cells in SYMP individuals:

We next studied the effect of blocking LAG-3 and PD-1 exhaustion pathways *ex vivo*, on the frequency and functionality of HSV-specific $CD8^+$ T cells. PBMCs from ASYMP and SYMP individuals were stimulated with the $VP11/12_{220–228}$ peptide (“RLNELLAYV”) and then pulsed with α-LAG-3 or α-PD-1 antagonist mAbs, with a combination of both mAbs, or with an isotype control mAb.

The α-LAG-3 mAbs significantly reduced the frequency of HSV-1 $VP11/12_{220–228}$-specific LAG-3^+CD8^+ T cells from both SYMP and ASYMP individuals (decreased from ~40–50% to ~10–20% LAG-3^+CD8^+ cells in SYMP and from ~15–20% to ~4–10% in ASYMP individuals) (Fig. 4A, *left* and *right panels*). Similar results were observed using the αPD-1 mAb which reduced the frequency of HSV-1 $VP11/12_{220–228}$-specific PD-1^+CD8^+ T cells from ~60% to ~30–40% in SYMP and from ~40% to 25–30% in ASYMP individuals (Fig. 4A, *left* and *right panels*). Moreover, the combination of both α-LAG-3 and αPD-1 mAbs synergistically reduced the frequency of LAG-3^+CD8^+ cells to ~5–10% in SYMP and to ~0% in ASYMP individuals. The same combination synergistically reduced the frequency of PD-1^+CD8^+ cells to ~15–25% in SYMP and to~10–20% in ASYMP individuals (Fig. 4A, *left* and *right panels*). Accordingly, as shown in Fig. 4B, a significant reduction in the expression levels of LAG-3 and PD-1 exhaustion markers was detected at the surface of the HSV-specific $CD8^+$ T cells following blockade with α-LAG-3, α-PD-1, or the combination of both mAbs.

Furthermore, as illustrated in Fig. 4C, LAG-3 blockade alone increased the percentages of functional $VP11/12_{220–228}$-specific IFN-γ^+CD8^+ T cells from ~8–10% to 15–20% in SYMP individuals (P<0.001). This same blockade alone also increased the percentages of degranulation-capable $VP11/12_{220–228}$-specific $CD107^+CD8^+$ T cells from ~4–6% to 12–15% in SYMP individuals (P<0.001). A similar trend was obtained with PD-1 blockade alone in SYMP individuals (percentages of $VP11/12_{220–228}$-specific IFN-γ^+CD8^+ T cells and $VP11/12_{220–228}$-specific $CD107^+CD8^+$ T cells increased to up to ~12–18% and 9–16% after blockade, respectively). Moreover, the combination of both α-LAG-3 and α-PD-1 mAbs had a synergistic positive effect on the function of HSV-specific $CD8^+$ T cells from SYMP individuals: this combination of blocking mAbs induced significantly higher

Author Manuscript Author Manuscript Author Manuscript Author Manuscript

percentages of VP11/12$_{220–228}$-specific IFN-γ^+CD8$^+$ T cells compared to the blockade of either PD-1 or LAG-3 pathways alone (~20–30% vs. 12–18% of IFN-γ^+CD8$^+$ T cells with PD-1 alone, or 15–20% with LAG-3 alone – P <0.05). Similar to HSV-specific CD8$^+$ T cells from SYMP individuals, we also observed improved function of HSV-specific CD8$^+$ T cells from ASYMP individuals following α-LAG-3 and/or α-PD-1 blockade (Fig. 4C), with the same synergistic effect (~35% vs. 25% of IFN-γ^+CD8$^+$ T cells). However, the synergistic effect was not observed for CD107$^{a/b+}$CD8$^+$ T cells (Fig. 4C).

Taken together, these results suggest that combination blockade of LAG-3 and PD-1 immune checkpoints appears to synergistically work together to successfully restore the function of exhausted HSV-specific CD8$^+$ T cells from SYMP individuals. Indeed, after blockade, the percentage of cells expressing IFN-γ and with degranulation ability in HSV-specific CD8$^+$ T cells from SYMP patients reached the same percentage than in ASYMP individuals without any treatment.

Due to ethical and practical complexities in obtaining draining lymph-nodes, cornea and trigeminal ganglia (TG) in humans, we were limited to studying blood-derived HSV-specific $^+$ T cells. However, the phenotype and function of blood-derived CD8$^+$ T cells may not reflect the phenotype and function of lymph node- and tissue-resident CD8$^+$ T cells. Hence, the remainder of this study utilized our established HLA-A*02:01 transgenic (Tg) mouse model of ocular herpes to determine whether blockade of various immune checkpoints (i.e. PD-1, LAG-3, TIGIT and TIM-3) would produce functional CD8$^+$ T cells that will protect from ocular herpes infection and disease.

5. Blockade of LAG-3 and PD-1 restored the function of anti-viral CD8$^+$ T cell responses and reduced recurrent ocular herpes in HSV-1 infected HLA-A*0201 transgenic mice:

We next studied the effect of blocking LAG-3 and PD-1 using antagonist mAbs, on recurrent ocular herpes infection, disease and anti-viral CD8$^+$ T cell responses. As illustrated in Fig. 5A, a total of 40 HLA-A*0201 Tg mice were infected with HSV-1 (2×10^5 pfu of strain McKrae). On day 35 post infection (i.e. during latency), all mice were subjected to UV-B induced HSV-1 reactivation. Subsequently, animals then received an I.P. injection of α-PD-1, α-LAG-3, a combination of both α-PD-1 and α-LAG-3 mAbs or an isotype control mAb (n = 10/group) on days 3, 5 and 7 post UV-B exposure (i.e. days 37, 39 and 41 post infection, respectively).

Following α-PD-1 or α-LAG-3 blockade, there was a significant decrease in cumulative recurrent keratitis (P < 0.05, Fig. 5B). Moreover, the combination of α-PD-1 and α-LAG-3 mAbs had a synergistic effect on recurrent corneal disease. This was associated to a significant decrease in the severity of recurrent ocular disease (Fig. 5C) and to a significant reduction in virus titers (Fig. 5D). The α-PD-1 and/or α-LAG-3 blockade resulted in a significant decrease in the severity of UV-B-induced recurrent ocular disease, as represented by cornea disease pictures, as illustrated in Fig. 5E.

Furthermore, following the gating strategy illustrated in Fig. S2, we observed a significant increase in the frequency of functional HSV-1 VP11/12$_{220–228}$-specific CD8$^+$ T cells detected in both cornea (Fig. 5F) and TG (Fig. 5G) of αLAG-3 and αPD-1 mAb treated

Author Manuscript Author Manuscript Author Manuscript Author Manuscript

mice as compared to non-treated mice. The frequencies of $VP11/12_{220–228}$-specific IFN-γ^+CD8^+ T cells, $CD107^+CD8^+$ T cells, and Ki-67^+CD8^+ T cells were all increased in αLAG-3 and αPD-1 mAb-treated groups compared to the isotype control group. Moreover, a synergistic effect of the combination of both antibodies was also observed (Fig. 5F and 5G). No systemic or local side effects were detected following the blockade of both the LAG-3 and PD-1 pathways. Unlike in B6 mice where 50% to 60% of HSV-specific $CD8^+$ T cells appeared to be directed to a single epitope $gB_{495–505}$, our HLA-A*0201 transgenic mice are not directed against a single human epitope such as $VP11/12_{220–228}$. Therefore, the $VP11/12_{220–228}$ is not the only immunodominant $CD8^+$-T cell epitope in McKrae latently infected HLA-A*0201 transgenic mice. However, $CD8^+$-T cells specific to other HSV-1 HLA-A*0201-restricted epitopes are also functionally affected in both humans (Fig. S2) and HLA-A*0201 transgenic mice.

Altogether, these results confirmed that blockade of the LAG-3 and PD-1 exhaustion pathways safely and efficiently reversed functional exhaustion of HSV-specific $CD8^+$ T cells associated to a reduction in recurrent ocular herpes disease in HSV-1 infected HLA-A*0201 transgenic mice.

6. Restoration of function of HSV-specific $CD8^+$ T cells associated to a reduction of virus reactivation from HSV-1 infected trigeminal ganglia following synergistic blockade of PD-1 and LAG-3 immune checkpoints:

Since *in vivo* blockade immune checkpoints restored the frequency and function of TG-resident $CD8^+$ T cells in latently infected mice, we next assessed whether such a blockade would also affect virus reactivation from TG explants.

HLA-A*0201 Tg mice (n =10) were ocularly infected with HSV-1 (2.5×10^5 pfu/eye, lab strain McKrae). The exhaustion status of HSV-specific $CD8^+$ T cells collected from DLN on day 14 post-ocular infection was determined using the gating strategy as illustrated in Fig. S3. Consistent with our results in human blood-derived $CD8^+$ T cells, mice $VP11/12_{220–228}$-specific $CD8^+$ T cells collected from the DLN expressed PD-1 (23%) and LAG-3 (32%) exhaustion markers (Fig. 6A). However, the expression levels of those markers dramatically diminished upon the addition of blocking mAbs to T cell cultures *ex vivo*. Pulsing DLN-derived $CD8^+$ T cells *ex vivo* with just 10 μg/mL of α-PD-1 mAb for two days resulted in a~2-fold decrease in both MFI and percentages of $CD8^+$ T cells expressing PD-1 (from 23% –MFI=203; to 11% –MFI=95) and LAG-3 (from 32% –MFI=679; to 14.5% –MFI=305). In addition, the effect of α-PD-1 and α-LAG-3 blocking mAbs was dose-dependent with a higher effect obtained with a 30 μg/mL.

We next examined the effect of α-PD-1 and α-LAG-3 antagonist mAbs on the function of DLN-resident $VP11/12_{220–228}$-specific $CD8^+$ T cells by measuring their ability to produce IFN-γ, $CD107^{a/b}$ and Ki-67 (Fig. 6B). Consistent with our aforementioned human results, the frequencies of mouse IFN-γ^+CD8^+, $CD107^{a/b+}CD8^+$ and Ki-67^+CD8^+ T cells significantly increased (P<0.001) following *ex vivo* incubation with α-PD-1 or α-LAG-3 blocking mAbs, in a dose-response manner (Fig 6B – *right and left panels*). The increase in the frequency of functional HSV-specific $CD8^+$ T cells was particularly pronounced with 30 μg/mL of αLAG-3 blockade resulting in more functional $CD8^+$ T cells compared to other

Author Manuscript Author Manuscript Author Manuscript Author Manuscript

mAbs blockade and to the isotype control (18.0% IFN-γ^{+}CD8^{+} T cells, 36.6% CD107$^{a/b+}$CD8^{+} T cells and 12.2% Ki-67^{+}CD8^{+} T cells) (Fig 6B – *right and left panels*).

Fourteen days post-infection, trigeminal ganglia TG were extracted, finely chopped and cell suspension were placed in culture with or without α-PD-1, α-PDL-1, α-LAG-3, α-CD8, α-IFN-γ and its receptor, with a combination of mAbs or with an isotype control mAb. The amount of reactivated virus was assessed in tissue culture on daily for 8 days post-treatment (Fig. 6C).

Significant effects were observed 6 days after treatment with α-PD-1 or α-LAG-3 blocking mAbs, where the amount of reactivated virus significantly decreased from HSV-1 infected TG explants by ~4–5 fold compared to isotype control (Fig. 6C, $P < 0.05$). Blocking PDL-1, the ligand of PD-1, also slightly reduced the amount of reactivated virus at day 6 post explant. The combination of α-LAG-3 and α-PD-1 depicted a synergistic effect on day 6. Regardless of the mAbs used, there was no significant difference in the amount of reactivated virus at days 4 post-treatment and only α-LAG-3 alone or α-PD-1 + α-LAG-3 together both significantly reduced the reactivation of HSV-1 in TG at day 8 post explant. As expected, the blockade of CD8^{+}, IFN-γ or IFN-R resulted in a significant increase in viral reactivation from HSV-1 infected TG explants, confirming the role of the IFN-γ−producing CD8^{+} T cells in controlling HSV-1 reactivation.

Overall, our mouse results; (*i*) confirmed the human data above, by demonstrating restoration of functional HSV-specific CD8^{+} T cells following blockade of the PD-1 and LAG-3 immune checkpoints and (*ii*) demonstrated that blockade of these PD-1 and LAG-3 immune checkpoints resulted in reduced virus reactivation *ex vivo* from HSV-1 infected TG, ultimately resulting in the therapeutic effect of α-PD-1 and α-LAG-3 against recurrent ocular herpes (Fig. 5).

DISCUSSION

A staggering 3.72 billion individuals worldwide are infected, often latently, with herpes simplex virus type 1 (HSV-1), a prevalent human viral pathogen (2, 40, 41). In symptomatic individuals, HSV-1 reactivation from latency causes complications which range from mild, such as cold sores and genital lesions, to grave, such as permanent brain damage from encephalitis, and blinding recurrent corneal herpetic disease (42). An immunotherapeutic strategy is currently not available for recurrent ocular herpes. The cross-talk between reactivated HSV-1 and local TG-resident antiviral CD8^{+} T cells contributes to control latency/reactivation cycles. In the present study, we demonstrated that: (*i*) Genes associated to multiple T cell exhaustion pathways were up-regulated in HSV-specific CD8^{+} T cells from symptomatic herpes patients; (*ii*) PD-1, LAG-3, TIGIT and TIM-3 exhaustion receptors were up-regulated on the surface of HSV-specific CD8^{+} T cells from symptomatic herpes patients; (*iii*) Multiple exhaustion receptors were co-expressed on the surface of dysfunctional HSV-specific CD8^{+} T cells detected from symptomatic herpes patients; (*iv*) Blockade of LAG-3 and/or PD-1 immune checkpoints restored the frequency and function of HSV-specific CD8^{+} T cells in SYMP individuals; (*v*) Restoration of functional of HSV-specific CD8^{+} T cells following *ex vivo* blockade of PD-1 and LAG-3 immune checkpoints

Author Manuscript Author Manuscript Author Manuscript Author Manuscript

was confirmed *in vivo* in HSV-1 infected HLA-A*0201 transgenic mice; (*vi*) Blockade of LAG-3 and PD-1 strengthens the anti-viral $CD8^+$ T cell responses and reduces recurrent ocular herpes in HSV-1 infected HLA-A*0201 transgenic mice; and (*vii*) Reduction of virus reactivation from HSV-1 infected TG following *ex vivo* blockade of PD-1 and LAG-3 immune checkpoints. In the present study, we showed that restoring the functionality of exhausted HSV-specific $CD8^+$ T cells following PD1/LAG3 mAbs blockade is associated with low frequency of virus reactivation in TG explants. Moreover, the treated mice had less severe recurrent HSK following UV-B-induce reactivation. It is likely the PD1/LAG3 mAbs blockade *in vivo* affected the functionally of $CD4^+$ T cells, immune cells reported in orchestrating HSK disease. Overall this report confirmed the coregulation of antiviral $CD8^+$ T cell exhaustion by multiple inhibitory receptors during symptomatic herpes infection.

Persistent viral infections are characterized as those in which the virus is not cleared, but remains in specific immune or non-immune cells of infected host cells. One fundamental question from the present report is whether viruses from the alpha herpesvirus family do indeed use T cell exhaustion as an immune evasion mechanism for survival (43–47). Persistent infections may involve stages of both silent (i.e. latent) and productive infection, without rapidly killing or even producing excessive damage to the host's cells (48). There are three major and overlapping types of persistent viral infections: (1) Latent infection that is characterized by the lack of demonstrable infectious virus following primary infection and between episodes of recurrent disease, (2) Chronic infection that is characterized by the continued presence of infectious virus following the primary infection; and (3) Slow infection that is characterized by a prolonged incubation period followed by progressive disease. Persisting chronic viral infections, such as with LCMV, HCV, HBV or even HIV, are often associated with continuous T cell activation leading to phenotypic and functional exhaustion of $CD4^+$ and $CD8^+$ effector T cells (49, 50). Whether such T cell exhaustion occurs during infections with alpha herpes viruses, such as HSV-1, remains controversial. Reports which tend to deny that HSV-1 infection induced T cell exhaustion as an immune evasion mechanism for survival were performed in mouse models of primary HSV-1 infections, models in which the phenotype and function of HSV-specific T cells may not represent the exhaustion of HSV-specific T cells as it occurs in humans during recurrent HSV-1 infections (43, 51). Following primary infection, HSV-1 establishes latent infection in ganglionic neurons where, except for the expression of the latency-associated transcripts (LAT), the expression of all other viral genes (and viral antigens) are supposed to be shut down (52). However, one recent study indicates that the expression of lytic genes is frequent during HSV-1 latency and correlates with the engagement of a cell-intrinsic transcriptional response (53). These findings, with the current study, suggest that instead of being a latent infection, HSV-1 infection may in fact be a chronic infection. The continued presence of infectious virus (and hence of viral antigens) following repetitive reactivations may cause exhaustion of $CD8^+$ effector T cells. Unlike in mouse models of primary HSV-1 infection, in humans, the virus continuously and spontaneously reactivates from latency leading to symptomatic or asymptomatic shedding (51, 54, 55).

The phenotype and function of epitope-specific $CD8^+$ T cells dominant HLA-A*0201-restricted epitope in the VZV ribonucleotide reductase subunit 2 was analyzed. Interestingly, $CD8^+$ T cells responding to this VZV epitope also recognized homologous epitopes, not

Author Manuscript Author Manuscript Author Manuscript Author Manuscript

only in the other alpha-herpesviruses, HSV-1 and HSV-2, but also the gamma-herpesvirus, EBV (56). $CD8^+$ T cell responses against these epitopes did not depend on previous infection with the originating virus, thus indicating the cross-reactive nature of this T cell population. Between individuals, the cells demonstrated marked phenotypic heterogeneity. This was associated with differences in functional capacity related to increased inhibitory receptor expression (including PD-1) along with decreased expression of co-stimulatory molecules that potentially reflected their stimulation history.

It is likely that the cross-reactivity between T cells epitopes of HSV-1 and HSV-2 and VZV, known as heterologous immunity, may have shaped the exhaustion of HSV-specific $CD8^+$ T cells observed in the herpes simplex symptomatic subjects analyzed in this study since cross-reactive epitopes between HSV-1 and HSV-2 and VZV have been reported (56). Nevertheless, since our HLA transgenic mice are of HLA-A*0201 haplotype, it is likely that the later haplotype is mostly involved in the HSV-1 epitope presentation.

The concept of blocking immune checkpoints first arose in cancer systems back to the 1990s, where James P. Allison and Tasuku Honjo described the fundamental role of PD-1 and CTLA-4 costimulatory receptors in T cell exhaustion (57, 58). Expression of PD-1 or CTLA-4 receptors was shown to be up-regulated at the surface of tumor-infiltrating T cells and blocking those inhibitory receptors using specific antagonist mAbs reversed T cells exhaustion associated with a reduction of tumors (59, 60). The recent success of therapies targeting immune checkpoints to treat many cancers has driven a reappearance of interest in therapies targeting immune checkpoints against chronic infections and diseases (20, 27, 31, 50, 61–75). Due to side effects associated to systemic delivery of immune checkpoint inhibitors, the neurotropic viruses, such as HSV-1, has been suggested as a vectors for local delivery of immune checkpoint inhibitors to treat many cancers (76). In light of the present study demonstrating induction of multiple exhaustion pathways, one would question the usefulness of HSV-1 as a vector for cancer immunotherapy.

The mechanisms driving $CD8^+$ T cells exhaustion during HSV-1 infection remain to be elucidated (77). Several factors may contribute to functional exhaustion of HSV-specific $CD8^+$ T cells including the amount of viral antigens, which is determined by the persistence and chronicity of HSV-1 infection, the extent and pace of viral reactivation and replication; the availability of $CD4^+$ T cell help; the strength of the natural killer cell response; the APC populations; and the levels and the composition of the cytokine milieu (63, 77). Metabolic dysregulation, uncontrolled inflammation and poor homeostatic self-renewal are also linked with expression of exhaustion receptors that contribute significantly to the development of T cell exhaustion (77–79). HSV-specific $CD8^+$ T cell response (in a cross talk with the neurons and the virus LAT gene) is closely involved in preventing viral reactivation from latency (6, 21–25). We previously reported that the expression of the LAT gene by latently infected sensory neurons (38, 80) was associated to exhaustion of TG-resident HSV-specific $CD8^+$ T cells in mice and rabbits (6, 25). Thus, controlling chronic HSV infections by testing different therapeutic vaccine strategies combined with various immune checkpoint blockades to restore the functional state of the HSV-specific $CD8^+$ T cells is an emerging possibility (14, 20, 27, 81). To develop an effective therapeutic vaccine, one would steer the T cells immune response from the SYMP patients to the one observed in ASYMP

Author Manuscript Author Manuscript Author Manuscript Author Manuscript

individuals. In the present study we found a reduction of virus reactivation from HSV-1 infected TG explants following *ex vivo* blockade of PD-1 and LAG-3 immune checkpoints. This was associated with a restoration of the function of local HSV-specific $CD8^+$ T cells, measured by their ability to produce IFN-γ and to degranulate, with yet-to-be determined mechanisms.

While the role of $CD8^+$ T cells in the control of herpes simplex virus type 1 (HSV-1) infection and disease has become important recently, a direct involvement of effector $CD4^+$ T cells in protection and immunopathology is gaining wider acceptance (82). Activated $CD4^+$ T cells are retained in latently infected trigeminal ganglia (TG) of mice and humans. Besides their direct effect on virus replication, the $CD4^+$ T helper cells are a source of large amounts of cytokines that promote the generation of primary and memory $CD8^+$ T cell responses, thus indirectly contributing to protection (83, 84). Although cornea-resident $CD4^+$ T cells have been reported as being involved in immunopathology of HSK mouse models of ocular herpes (85, 86) the involvement of $CD4^+$ T cells retained in cornea of humans with HSK has not yet been reported.

We found the expression of genes associated to various cytokine pathways, such as IL-2, IL-7 and IL-15, to be down-regulated in HSV-specific $CD8^+$ T cells from SYMP compared to ASYMP individuals in agreement with other reports on chronic viral infection (31). IL-2 controls expansion and differentiation of antiviral $CD8^+$ T cells, whereas IL-7 and IL-15 are central in maintaining memory $CD8^+$ T cells. The exact functions of IL-2, IL-7 and IL-15 cytokines during HSV-1 recurrent infection remains to be fully elucidated. In other chronic infections, administration of IL-2, IL-7, or IL-15 can increase the function of exhausted $CD8^+$ T cells (62, 87), others have showed that IL2Rβ, common to both IL15-R and IL-2R, is expressed on terminally exhausted HSV-specific $CD8^+$ T cells depicting IL-2 and IL-15 – but not IL-7, as instigators of $CD8^+$ T cell exhaustion in this particular context (88). Nonetheless, in the context of HSV-1 infection genes coding for IL-7R(α), IL-15, IL-2 and IL-2Rβ were less expressed in HSV-specific $CD8^+$ T cells from SYMP individuals compared to ASYMP, whereas IL-2Rα (CD25) was upregulated. Deficiencies in cytokine signaling seemed not confined to expression of cell-surface receptors since we depict a JAK/STAT pathway defect in HSV-specific $CD8^+$ T cells from SYMP individuals (in which JAK1, JAK2 and STAT5B, along with IL-2, IL-4R, IL-6ST and IL-7R transcripts are under expressed. This is in line with our previous report in the context of HSV-1 infection (29) and by others reports in the context of chronic viral infections (31).

Several transcription factor genes were differently expressed by HSV-specific $CD8^+$ T cells from SYMP compared to ASYMP individuals. For instance, we found that both Fos and FosB genes were less expressed in HSV-specific $CD8^+$ T cells from SYMP individuals compared to those of the ASYMP individuals. Previous reports indicate that Fos and FosB, components of the dimeric transcription factor AP-1, exhibit low expression in exhausted LCMV-specific T cells (31). The Klf1, Klf2 and Klf3 transcription factors were also downregulated at the mRNA level in HSV-specific $CD8^+$ T cells, confirming previous report in LCMV-specific $CD8^+$ T cells (31). A lack of Klf2 expression, in particular, has been linked to default in T cell quiescence and migration (89). Furthermore, we found a significant lower expression of the *ACSS1* gene in HSV-specific $CD8^+$ T cells from SYMP

Author Manuscript Author Manuscript Author Manuscript Author Manuscript

compared to ASYMP individuals. Since we also found a lower expression of IFN-γ in HSV-specific $CD8^+$ T cells from SYMP individuals, both at the gene and protein levels, these results are in line with a recent report showing that acetate promotes histone acetylation and chromatin accessibility and enhances IFN-γ gene transcription and cytokine production in $CD8^+$ T cells in an acetyl-CoA synthetase (ACSS1)-dependent manner (90). We also found genes for *4–1BB* (TNFSFR9 transcript) to be downregulated in HSV-specific $CD8^+$ T cells from SYMP compared to ASYMP individuals. Genes for 4–1BB (TNFSFR9) transcription factor, a co-stimulatory receptor (91), synergized with PD-1 blockade to restore the T cells functions during LCMV chronic infection (92). Thus, it would be interesting to test the combination of 4–1BB agonist with the blocking of inhibitory receptors PD-1 and LAG-3 in HSV-1 infected animals. Interestingly, a decreased expression of *RABAC1* gene, described to be altered in exhausted T cells (31) was observed in HSV-specific $CD8^+$ T cells from SYMP compared to ASYMP individuals. PRAF1, the protein coded by *RABAC1*, is localized to Golgi and late endosomes. As part of the SNARE complex, PRAF1 may function either in the regulation of docking and fusion of transport vesicles at the plasma membrane, or as a sorting protein in the Golgi complex (93). Another protein, granzyme B, is a key molecule for the cytotoxicity of the $CD8^+$ T cells and plays a major role in preventing HSV-1 reactivation from neuronal latency by degrading the viral protein ICP4. Surprisingly, GzmB mRNA remains expressed by exhausted $CD8^+$ T cells in LCMV chronic infections (31). In agreement with this, we found a higher expression of GzmB mRNA in HSV-specific $CD8^+$ T cells from SYMP compared to ASYMP individuals. Although this seems counterintuitive with a loss of function, one hypothesis would be that the deficiency in the degranulation ability of the HSV-1 $CD8^+$ T cells which we measured both at the mRNA and the protein level in SYMP patients may explain the inability of these cells to release GzmB effectively. The differences observed between the $CD8^+$ bulk RNAseq results presented in panels C/D and the CD8 Nanostring results presented in panel E may be due to: (i) different statistical power used in each of these two methods; and (*ii*) the fact that the bulk RNAseq method allows us to determine differential gene expression in the HSV-specific $CD8^+$ T cell populations in an unbiased way, while the Nanostring method allows us to determine differential gene expression in pre-selected 579 immune genes.

In the present study, we discovered that genes associated to multiple T cell exhaustion receptors (PD-1, LAG-3, TIGIT and TIM-3) were up-regulated in HSV-specific $CD8^+$ T cells from symptomatic herpetic patients. Moreover, in symptomatic patients only, these multiple exhaustion receptors are co-expressed on the surface of dysfunctional HSV-specific $CD8^+$ T cells, and this was associated with functional impairment of these cells. Similarly, antiviral $CD8^+$ T cells in various chronic viral infections (i.e. HIV, HSV, HCV, HBV and LCMV) often express one or multiple exhaustion receptors (20, 27, 94), but more importantly co-expression of multiple exhaustion receptors is correlated with a gradual loss of function (20, 27, 31, 61, 63). We also demonstrated that blockade of LAG-3 and/or PD-1 immune checkpoints strengthened the anti-viral $CD8^+$ T cell responses and reduces recurrent ocular herpes in HSV-1 infected HLA-A*0201 transgenic mice. These findings confirm and extend our previous report in C57BL/6 mice and in HLA Tg rabbits (27, 95). Immune checkpoints are often divided into a first- and a second-generation. The first-generation checkpoints are PD-1/PD-L1 and CTLA-4, and the classic examples of the second-

Author Manuscript Author Manuscript Author Manuscript Author Manuscript

generation checkpoints are LAG-3, TIGIT, TIM-3, BTLA, CD160, PSGL-1, Ly49 and GITR. While blocking of the first-generation molecules is currently widely used, a recent shift placing focus toward targeting the second-generation molecules is noteworthy, as resistance to first generation therapies are amply reported and a combination of the two show synergistic and non-redundant effects (20, 33, 94, 96–98). This seems to be the case during HSV-1 infection where expression of multiple exhaustion receptors that likely caused HSV-specific $CD8^+$ T cells to gradually lose their polyfunctionality, culminating in T cell exhaustion (11, 20, 29, 99–101). However, little if any studies on the immune checkpoint blockade in the context of recurrent herpetic disease has focused on humans, but rather used animal models of primary herpes infection (6, 20, 25, 27, 80, 102).

To our knowledge, this is the first report to show that PD-1 and LAG-3 as well as TIGIT and TIM-3, are important immune checkpoint targets to restore TG-resident $CD8^+$ T cells and reduce herpes reactivation. Both PD-1 and LAG-3 pathways are likely to play a pivotal role in human recurrent herpes infection and according to our results, we are currently testing the effect of the blockade of TIGIT and TIM-3 in our animal models. Overall, this study indicates that T cell exhaustion also occurs during infections with alpha herpes viruses, such as HSV-1. Although the mechanisms driving $CD8^+$ T cells exhaustion during HSV-1 infection remains to be elucidated, the present report opens a new avenue towards therapeutic strategies targeting immune checkpoints, such as PD-1 and LAG-3 to treat recurrent herpetic disease.

Supplementary Material

Refer to Web version on PubMed Central for supplementary material.

ACKNOWLEDGEMENTS

This work is dedicated to the memory of late Professor Steven L. Wechsler “Steve” (1948–2016), whose numerous pioneering works on herpes infection and immunity laid the foundation to this line of research. We thank the NIH Tetramer Facility (Emory University, Atlanta, GA) for providing the Tetramers used in this study; Diane Capobianco (RN) from UC Irvine’s Institute for Clinical and Translational Science (ICTS) for helping with blood drawing from HSV-1 seropositive symptomatic & asymptomatic individuals. We also thank Angele Nalbandian, PhD. for her help editing this manuscript, Vanessa Scarfone for her help with the cell sorting and Melanie Oakes, PhD. for her advice on RNASeq data analysis (all are from University of California Irvine, Irvine, CA).

This work is supported by Public Health Service Research Grants EY026103, EY019896 and EY024618 from the National Eye Institute (NEI) and Grants AI150091, AI143348, AI147499, AI143326, AI138764, AI124911 and AI110902 from the National Institute of Allergy and Infectious Diseases (NIAID) and in part by The Discovery Center for Eye Research (DCER) and the Research to Prevent Blindness (RPB) grant.

REFERENCES

1. Looker KJ et al., Global and Regional Estimates of Prevalent and Incident Herpes Simplex Virus Type 1 Infections in 2012. PLoS One 10, e0140765–e0140765 (2015). [PubMed: 26510007]
2. Samandary S et al., Associations of HLA-A, HLA-B and HLA-C alleles frequency with prevalence of herpes simplex virus infections and diseases across global populations: implication for the development of an universal CD8+ T-cell epitope-based vaccine. Hum Immunol 75, 715–729 (2014). [PubMed: 24798939]
3. Johnston C, Wald A, Epidemiology, clinical manifestations, and diagnosis of herpes simplex virus type 1 infection.

Author Manuscript Author Manuscript Author Manuscript Author Manuscript

4. Ellermann-Eriksen S, Macrophages and cytokines in the early defence against herpes simplex virus. Virol J 2, 59 (2005). [PubMed: 16076403]
5. Cabrera JR, Charron AJ, Leib DA, Neuronal Subtype Determines Herpes Simplex Virus 1 Latency-Associated-Transcript Promoter Activity during Latency. J Virol 92, (2018).
6. Allen SJ et al., The role of LAT in increased CD8+ T cell exhaustion in trigeminal ganglia of mice latently infected with herpes simplex virus 1. J Virol 85, 4184–4197 (2011). [PubMed: 21307196]
7. Knickelbein JE et al., Noncytotoxic lytic granule-mediated CD8+ T cell inhibition of HSV-1 reactivation from neuronal latency. Science 322, 268–271 (2008). [PubMed: 18845757]
8. BenMohamed L et al., Decreased reactivation of a herpes simplex virus type 1 (HSV-1) latency-associated transcript (LAT) mutant using the in vivo mouse UV-B model of induced reactivation. Journal of neurovirology 21, 508–517 (2015). [PubMed: 26002839]
9. Grinde B, Herpesviruses: latency and reactivation - viral strategies and host response. J Oral Microbiol 5, (2013).
10. Dervillez X et al., Asymptomatic HLA-A*02:01-restricted epitopes from herpes simplex virus glycoprotein B preferentially recall polyfunctional CD8+ T cells from seropositive asymptomatic individuals and protect HLA transgenic mice against ocular herpes. J Immunol 191, 5124–5138 (2013). [PubMed: 24101547]
11. Srivastava R et al., Human Asymptomatic Epitopes Identified from the Herpes Simplex Virus Tegument Protein VP13/14 (UL47) Preferentially Recall Polyfunctional Effector Memory CD44high CD62Llow CD8+ TEM Cells and Protect Humanized HLA-A*02:01 Transgenic Mice against Ocular Herpesvirus Infection. J Virol 91, (2017).
12. Coulon PG et al., NLRP3, NLRP12, and IFI16 Inflammasomes Induction and Caspase-1 Activation Triggered by Virulent HSV-1 Strains Are Associated With Severe Corneal Inflammatory Herpetic Disease. Front Immunol 10, 1631 (2019). [PubMed: 31367214]
13. Farooq AV, Shukla D, Herpes simplex epithelial and stromal keratitis: an epidemiologic update. Surv Ophthalmol 57, 448–462 (2012). [PubMed: 22542912]
14. Chentoufi AA, Kritzer E, Yu DM, Nesburn AB, Benmohamed L, Towards a rational design of an asymptomatic clinical herpes vaccine: the old, the new, and the unknown. Clin Dev Immunol 2012, 187585 (2012). [PubMed: 22548113]
15. Wasmuth S, Bauer D, Yang Y, Steuhl KP, Heiligenhaus A, Topical treatment with antisense oligonucleotides targeting tumor necrosis factor-alpha in herpetic stromal keratitis. Invest Ophthalmol Vis Sci 44, 5228–5234 (2003). [PubMed: 14638721]
16. Sergerie Y, Boivin G, Gosselin D, Rivest S, Delayed but not early glucocorticoid treatment protects the host during experimental herpes simplex virus encephalitis in mice. J Infect Dis 195, 817–825 (2007). [PubMed: 17299711]
17. Tumpey TM, Elner VM, Chen SH, Oakes JE, Lausch RN, Interleukin-10 treatment can suppress stromal keratitis induced by herpes simplex virus type 1. J Immunol 153, 2258–2265 (1994). [PubMed: 8051423]
18. Chucair-Elliott AJ, Carr MM, Carr DJJ, Long-term consequences of topical dexamethasone treatment during acute corneal HSV-1 infection on the immune system. J Leukoc Biol 101, 1253–1261 (2017). [PubMed: 28115476]
19. St Leger AJ, Hendricks RL, CD8+ T cells patrol HSV-1-infected trigeminal ganglia and prevent viral reactivation. J Neurovirol 17, 528–534 (2011). [PubMed: 22161682]
20. Roy S et al., Blockade of PD-1 and LAG-3 Immune Checkpoints Combined with Vaccination Restores the Function of Antiviral Tissue-Resident CD8(+) TRM Cells and Reduces Ocular Herpes Simplex Infection and Disease in HLA Transgenic Rabbits. J Virol 93, (2019).
21. Khanna KM, Bonneau RH, Kinchington PR, Hendricks RL, Herpes simplex virus-specific memory CD8+ T cells are selectively activated and retained in latently infected sensory ganglia. Immunity 18, 593–603 (2003). [PubMed: 12753737]
22. Verjans GM et al., Selective retention of herpes simplex virus-specific T cells in latently infected human trigeminal ganglia. Proc Natl Acad Sci U S A 104, 3496–3501 (2007). [PubMed: 17360672]
23. Divito S, Cherpes TL, Hendricks RL, A triple entente: virus, neurons, and CD8+ T cells maintain HSV-1 latency. Immunol Res 36, 119–126 (2006). [PubMed: 17337772]

Author Manuscript Author Manuscript Author Manuscript Author Manuscript

24. Mott KR et al., Level of herpes simplex virus type 1 latency correlates with severity of corneal scarring and exhaustion of CD8+ T cells in trigeminal ganglia of latently infected mice. J Virol 83, 2246–2254 (2009). [PubMed: 19091870]
25. Srivastava R et al., The Herpes Simplex Virus Latency-Associated Transcript Gene Is Associated with a Broader Repertoire of Virus-Specific Exhausted CD8+ T Cells Retained within the Trigeminal Ganglia of Latently Infected HLA Transgenic Rabbits. Journal of Virology 90, 3913–3928 (2016). [PubMed: 26842468]
26. Hoshino Y, Pesnicak L, Cohen JI, Straus SE, Rates of reactivation of latent herpes simplex virus from mouse trigeminal ganglia ex vivo correlate directly with viral load and inversely with number of infiltrating CD8+ T cells. J Virol 81, 8157–8164 (2007). [PubMed: 17522198]
27. Roy S et al., Blockade of LAG-3 Immune Checkpoint Combined With Therapeutic Vaccination Restore the Function of Tissue-Resident Anti-viral CD8(+) T Cells and Protect Against Recurrent Ocular Herpes Simplex Infection and Disease. Front Immunol 9, 2922 (2018). [PubMed: 30619285]
28. Yu W et al., Critical Role of Regulatory T Cells in the Latency and Stress-Induced Reactivation of HSV-1. Cell Rep 25, 2379–2389 e2373 (2018). [PubMed: 30485807]
29. Vahed H et al., Unique Type I Interferon, Expansion/Survival Cytokines, and JAK/STAT Gene Signatures of Multifunctional Herpes Simplex Virus-Specific Effector Memory CD8(+) TEM Cells Are Associated with Asymptomatic Herpes in Humans. J Virol 93, (2019).
30. Gatz SA, Pohla H, Schendel DJ, A PCR-SSP method to specifically select HLA-A*0201 individuals for immunotherapeutic studies. Tissue antigens 55, 532–547 (2000). [PubMed: 10902609]
31. Wherry EJ et al., Molecular signature of CD8+ T cell exhaustion during chronic viral infection. Immunity 27, 670–684 (2007). [PubMed: 17950003]
32. Herr W et al., Identification of naturally processed and HLA-presented Epstein–Barr virus peptides recognized by CD4+ or CD8+ T lymphocytes from human blood. Proceedings of the National Academy of Sciences 96, 12033–12038 (1999).
33. Matsuzaki J et al., Tumor-infiltrating NY-ESO-1-specific CD8+ T cells are negatively regulated by LAG-3 and PD-1 in human ovarian cancer. Proc Natl Acad Sci U S A 107, 7875–7880 (2010). [PubMed: 20385810]
34. Boucherma R et al., HLA-A*01:03, HLA-A*24:02, HLA-B*08:01, HLA-B*27:05, HLA-B*35:01, HLA-B*44:02, and HLA-C*07:01 monochain transgenic/H-2 class I null mice: novel versatile preclinical models of human T cell responses. J Immunol 191, 583–593 (2013). [PubMed: 23776170]
35. BenMohamed L et al., Induction of CTL response by a minimal epitope vaccine in HLA A*0201/DR1 transgenic mice: dependence on HLA class II restricted T(H) response. Hum Immunol 61, 764–779 (2000). [PubMed: 10980387]
36. Osorio Y, Ghiasi H, Recombinant herpes simplex virus type 1 (HSV-1) codelivering interleukin-12p35 as a molecular adjuvant enhances the protective immune response against ocular HSV-1 challenge. J Virol 79, 3297–3308 (2005). [PubMed: 15731224]
37. Khan AA et al., Bolstering the Number and Function of HSV-1-Specific CD8(+) Effector Memory T Cells and Tissue-Resident Memory T Cells in Latently Infected Trigeminal Ganglia Reduces Recurrent Ocular Herpes Infection and Disease. J Immunol 199, 186–203 (2017). [PubMed: 28539429]
38. Chentoufi AA et al., The herpes simplex virus type 1 latency-associated transcript inhibits phenotypic and functional maturation of dendritic cells. Viral Immunol 25, 204–215 (2012). [PubMed: 22512280]
39. Chentoufi AA et al., Asymptomatic human CD4+ cytotoxic T-cell epitopes identified from herpes simplex virus glycoprotein B. J Virol 82, 11792–11802 (2008). [PubMed: 18799581]
40. Srivastava R et al., HLA-A02:01-restricted epitopes identified from the herpes simplex virus tegument protein VP11/12 preferentially recall polyfunctional effector memory CD8+ T cells from seropositive asymptomatic individuals and protect humanized HLA-A*02:01 transgenic mice against ocular herpes. J Immunol 194, 2232–2248 (2015). [PubMed: 25617474]

Author Manuscript Author Manuscript Author Manuscript Author Manuscript

41. Srivastava R et al., CXCL17 Chemokine-Dependent Mobilization of CXCR8(+)CD8(+) Effector Memory and Tissue-Resident Memory T Cells in the Vaginal Mucosa Is Associated with Protection against Genital Herpes. J Immunol, (2018).
42. Agelidis AM, Shukla D, Cell entry mechanisms of HSV: what we have learned in recent years. Future virology 10, 1145–1154 (2015). [PubMed: 27066105]
43. Mackay LK et al., Maintenance of T Cell Function in the Face of Chronic Antigen Stimulation and Repeated Reactivation for a Latent Virus Infection. The Journal of Immunology 188, 2173–2178 (2012). [PubMed: 22271651]
44. Tronstein E et al., Genital shedding of herpes simplex virus among symptomatic and asymptomatic persons with HSV-2 infection. Jama 305, 1441–1449 (2011). [PubMed: 21486977]
45. Wald A et al., Reactivation of genital herpes simplex virus type 2 infection in asymptomatic seropositive persons. N Engl J Med 342, 844–850 (2000). [PubMed: 10727588]
46. Kaufman HE et al., HSV-1 DNA in tears and saliva of normal adults. Invest Ophthalmol Vis Sci 46, 241–247 (2005). [PubMed: 15623779]
47. Ramchandani M et al., Herpes Simplex Virus Type 1 Shedding in Tears and Nasal and Oral Mucosa of Healthy Adults. Sex Transm Dis 43, 756–760 (2016). [PubMed: 27835628]
48. Boldogh I, Albrecht T, Porter DD, in Medical Microbiology, th, Baron S, Eds. (Galveston (TX), 1996).
49. Frebel H, Richter K, Oxenius A, How chronic viral infections impact on antigen-specific T-cell responses. Eur J Immunol 40, 654–663 (2010). [PubMed: 20077405]
50. Saeidi A et al., T-Cell Exhaustion in Chronic Infections: Reversing the State of Exhaustion and Reinvigorating Optimal Protective Immune Responses. Front Immunol 9, 2569 (2018). [PubMed: 30473697]
51. Stuart PM, Keadle TL, Recurrent herpetic stromal keratitis in mice: a model for studying human HSK. Clin Dev Immunol 88, 72–78 (2012).
52. Margolis TP, Imai Y, Yang L, Vallas V, Krause PR, Herpes simplex virus type 2 (HSV-2) establishes latent infection in a different population of ganglionic neurons than HSV-1: role of latency-associated transcripts. J Virol 81, 1872–1878 (2007). [PubMed: 17151134]
53. Ma JZ, Russell TA, Spelman T, Carbone FR, Tscharke DC, Lytic gene expression is frequent in HSV-1 latent infection and correlates with the engagement of a cell-intrinsic transcriptional response. PLoS Pathog 10, e1004237 (2014). [PubMed: 25058429]
54. BenMohamed L et al., Prior Corneal Scarification and Injection of Immune Serum are not Required Before Ocular HSV-1 Infection for UV-B Induced Virus Reactivation and Recurrent Herpetic Corneal Disease in Latently Infected Mice Current Eye Resaerch, (2015).
55. Shimeld C, Whiteland JL, Nicholls SM, Easty DL, Hill TJ, Immune cell infiltration in corneas of mice with recurrent herpes simplex virus disease. J Gen Virol 77 (Pt 5), 977–985 (1996). [PubMed: 8609495]
56. Chiu C et al., Broadly reactive human CD8 T cells that recognize an epitope conserved between VZV, HSV and EBV. PLoS Pathog 10, e1004008 (2014). [PubMed: 24675761]
57. Ishida Y, Agata Y, Shibahara K, Honjo T, Induced expression of PD-1, a novel member of the immunoglobulin gene superfamily, upon programmed cell death. EMBO J 11, 3887–3895 (1992). [PubMed: 1396582]
58. Leach DR, Krummel MF, Allison JP, Enhancement of antitumor immunity by CTLA-4 blockade. Science 271, 1734–1736 (1996). [PubMed: 8596936]
59. Bazhin AV, Amedei A, Karakhanova S, Editorial: Immune Checkpoint Molecules and Cancer Immunotherapy. Front Immunol 9, 2878 (2018). [PubMed: 30568661]
60. Rotte A, D'Orazi G, Bhandaru M, Nobel committee honors tumor immunologists. J Exp Clin Cancer Res 37, 262 (2018). [PubMed: 30376854]
61. Wherry EJ, Blattman JN, Murali-Krishna K, van der Most R, Ahmed R, Viral persistence alters CD8 T-cell immunodominance and tissue distribution and results in distinct stages of functional impairment. J Virol 77, 4911–4927 (2003). [PubMed: 12663797]
62. Shin H, Wherry EJ, CD8 T cell dysfunction during chronic viral infection. Curr Opin Immunol 19, 408–415 (2007). [PubMed: 17656078]

Author Manuscript Author Manuscript Author Manuscript Author Manuscript

63. Kahan SM, Wherry EJ, Zajac AJ, T cell exhaustion during persistent viral infections. Virology 479–480, 180–193 (2015).
64. Youngblood B et al., Cutting edge: Prolonged exposure to HIV reinforces a poised epigenetic program for PD-1 expression in virus-specific CD8 T cells. J Immunol 191, 540–544 (2013). [PubMed: 23772031]
65. Freeman GJ, Wherry EJ, Ahmed R, Sharpe AH, Reinvigorating exhausted HIV-specific T cells via PD-1–PD-1 ligand blockade. Journal of Experimental Medicine 203, 2223–2227 (2006). [PubMed: 17000870]
66. Urbani S et al., PD-1 expression in acute hepatitis C virus (HCV) infection is associated with HCV-specific CD8 exhaustion. Journal of virology 80, 11398–11403 (2006). [PubMed: 16956940]
67. McMahan RH et al., Tim-3 expression on PD-1+ HCV-specific human CTLs is associated with viral persistence, and its blockade restores hepatocyte-directed in vitro cytotoxicity. The Journal of clinical investigation 120, 4546–4557 (2010). [PubMed: 21084749]
68. Nakamoto N et al., Functional restoration of HCV-specific CD8 T cells by PD-1 blockade is defined by PD-1 expression and compartmentalization. Gastroenterology 134, 1927–1937.e1922 (2008). [PubMed: 18549878]
69. Nakamoto N et al., Synergistic reversal of intrahepatic HCV-specific CD8 T cell exhaustion by combined PD-1/CTLA-4 blockade. PLoS pathogens 5, e1000313 (2009). [PubMed: 19247441]
70. Gane E et al., Anti-PD-1 blockade with nivolumab with and without therapeutic vaccination for virally suppressed chronic hepatitis B: A pilot study. J Hepatol 71, 900–907 (2019). [PubMed: 31306680]
71. Porichis F et al., Immune Checkpoint Blockade Restores HIV-Specific CD4 T Cell Help for NK Cells. J Immunol 201, 971–981 (2018). [PubMed: 29934472]
72. Grabmeier-Pfistershammer K et al., Antibodies targeting BTLA or TIM-3 enhance HIV-1 specific T cell responses in combination with PD-1 blockade. Clin Immunol 183, 167–173 (2017). [PubMed: 28882621]
73. Fujita T et al., Expansion of dysfunctional Tim-3-expressing effector memory CD8+ T cells during simian immunodeficiency virus infection in rhesus macaques. J Immunol 193, 5576–5583 (2014). [PubMed: 25348621]
74. Chew GM et al., TIGIT Marks Exhausted T Cells, Correlates with Disease Progression, and Serves as a Target for Immune Restoration in HIV and SIV Infection. PLoS Pathog 12, e1005349 (2016). [PubMed: 26741490]
75. Wykes MN, Lewin SR, Immune checkpoint blockade in infectious diseases. Nat Rev Immunol 18, 91–104 (2018). [PubMed: 28990586]
76. Sivanandam V, LaRocca CJ, Chen NG, Fong Y, Warner SG, Oncolytic Viruses and Immune Checkpoint Inhibition: The Best of Both Worlds. Mol Ther Oncolytics 13, 93–106 (2019). [PubMed: 31080879]
77. McLane LM, Abdel-Hakeem MS, Wherry EJ, CD8 T Cell Exhaustion During Chronic Viral Infection and Cancer. Annu Rev Immunol 37, 457–495 (2019). [PubMed: 30676822]
78. Staron MM et al., The transcription factor FoxO1 sustains expression of the inhibitory receptor PD-1 and survival of antiviral CD8(+) T cells during chronic infection. Immunity 41, 802–814 (2014). [PubMed: 25464856]
79. Bengsch B et al., Bioenergetic Insufficiencies Due to Metabolic Alterations Regulated by the Inhibitory Receptor PD-1 Are an Early Driver of CD8(+) T Cell Exhaustion. Immunity 45, 358–373 (2016). [PubMed: 27496729]
80. Chentoufi AA et al., The herpes simplex virus 1 latency-associated transcript promotes functional exhaustion of virus-specific CD8+ T cells in latently infected trigeminal ganglia: a novel immune evasion mechanism. J Virol 85, 9127–9138 (2011). [PubMed: 21715478]
81. Allen SJ, Mott KR, Zandian M, Ghiasi H, Immunization with different viral antigens alters the pattern of T cell exhaustion and latency in herpes simplex virus type 1-infected mice. J Virol 84, 12315–12324 (2010). [PubMed: 20861248]
82. Srivastava R et al., Human Epitopes Identified from Herpes Simplex Virus Tegument Protein VP11/12 (UL46) Recall Multifunctional Effector Memory CD4(+) TEM Cells in Asymptomatic

Author Manuscript Author Manuscript Author Manuscript Author Manuscript

Individuals and Protect from Ocular Herpes Infection and Disease in “Humanized” HLA-DR Transgenic Mice. J Virol 94, (2020).

83. Rajasagi NK et al., CD4+ T cells are required for the priming of CD8+ T cells following infection with herpes simplex virus type 1. J Virol 83, 5256–5268 (2009). [PubMed: 19279095]
84. Johnson AJ, Chu CF, Milligan GN, Effector CD4+ T cell involvement in clearance of infectious herpes simplex virus type 1 from sensory ganglia and spinal cords. J Virol, (2008).
85. Niemialtowski MG, Rouse BT, Predominance of Th1 cells in ocular tissues during herpetic stromal keratitis. J Immunol 149, 3035–3039 (1992). [PubMed: 1357034]
86. Doymaz MZ, Rouse BT, Herpetic stromal keratitis: an immunopathologic disease mediated by CD4+ T lymphocytes. Invest Ophthalmol Vis Sci 33, 2165–2173 (1992). [PubMed: 1351475]
87. Hashimoto M, Im SJ, Araki K, Ahmed R, Cytokine-Mediated Regulation of CD8 T-Cell Responses During Acute and Chronic Viral Infection. Cold Spring Harb Perspect Biol 11, (2019).
88. Beltra JC et al., IL2Rbeta-dependent signals drive terminal exhaustion and suppress memory development during chronic viral infection. Proc Natl Acad Sci U S A 113, E5444–5453 (2016). [PubMed: 27573835]
89. Carlson CM et al., Kruppel-like factor 2 regulates thymocyte and T-cell migration. Nature 442, 299 (2006). [PubMed: 16855590]
90. Qiu J et al., Acetate Promotes T Cell Effector Function during Glucose Restriction. Cell Rep 27, 2063–2074 e2065 (2019). [PubMed: 31091446]
91. Long AH et al., 4–1BB costimulation ameliorates T cell exhaustion induced by tonic signaling of chimeric antigen receptors. Nature medicine 21, 581 (2015).
92. Vezys V et al., 4–1BB signaling synergizes with programmed death ligand 1 blockade to augment CD8 T cell responses during chronic viral infection. The Journal of Immunology 187, 1634–1642 (2011). [PubMed: 21742975]
93. Compton SL, Behrend EN, PRAF1: a Golgi complex transmembrane protein that interacts with viruses. Biochem Cell Biol 84, 940–948 (2006). [PubMed: 17215881]
94. Blackburn SD et al., Coregulation of CD8+ T cell exhaustion by multiple inhibitory receptors during chronic viral infection. Nat Immunol 10, 29–37 (2009). [PubMed: 19043418]
95. Roy S et al., Blockade of PD-1 and LAG-3 Immune Checkpoints Combined with Vaccination Restore the Function of Anti-Viral Tissue-Resident CD8(+) TRM Cells and Reduce Ocular Herpes Simplex Infection and Disease in HLA Transgenic Rabbits. J Virol, (2019).
96. Chen JH et al., Prostaglandin E2 and programmed cell death 1 signaling coordinately impair CTL function and survival during chronic viral infection. Nat Med 21, 327–334 (2015). [PubMed: 25799228]
97. Woo S-R et al., Immune Inhibitory Molecules LAG-3 and PD-1 Synergistically Regulate T-cell Function to Promote Tumoral Immune Escape. Cancer Research 72, 917–927 (2012). [PubMed: 22186141]
98. Johnston RJ et al., The immunoreceptor TIGIT regulates antitumor and antiviral CD8(+) T cell effector function. Cancer Cell 26, 923–937 (2014). [PubMed: 25465800]
99. Frank GM et al., Early CD4(+) T cell help prevents partial CD8(+) T cell exhaustion and promotes maintenance of Herpes Simplex Virus 1 latency. J Immunol 184, 277–286 (2010). [PubMed: 19949087]
100. Wherry EJ, T cell exhaustion. Nature Immunology 12, 492–499 (2011). [PubMed: 21739672]
101. Srivastava R et al., Phenotypic and Functional Signatures of Herpes Simplex Virus-Specific Effector Memory CD73(+)CD45RA(high)CCR7(low)CD8(+) TEMRA and CD73(+)CD45RA(low)CCR7(low)CD8(+) TEM Cells Are Associated with Asymptomatic Ocular Herpes. J Immunol 201, 2315–2330 (2018). [PubMed: 30201808]
102. Khan AA et al., Therapeutic immunization with a mixture of herpes simplex virus 1 glycoprotein D-derived “asymptomatic” human CD8+ T-cell epitopes decreases spontaneous ocular shedding in latently infected HLA transgenic rabbits: association with low frequency of local PD-1+ TIM-3+ CD8+ exhausted T cells. J Virol 89, 6619–6632 (2015). [PubMed: 25878105]

Author Manuscript Author Manuscript Author Manuscript Author Manuscript

KEY POINTS:

- HSV-specific $CD8^+$ T cells from HSV-1 infected symptomatic patients are exhausted.
- Blocking of LAG-3 and PD-1 synergistically restored anti-HSV $CD8^+$ T cell responses.
- LAG-3 and PD-1 blockade reduced recurrent ocular herpes in HSV-1 infected mice.

Author Manuscript Author Manuscript Author Manuscript Author Manuscript

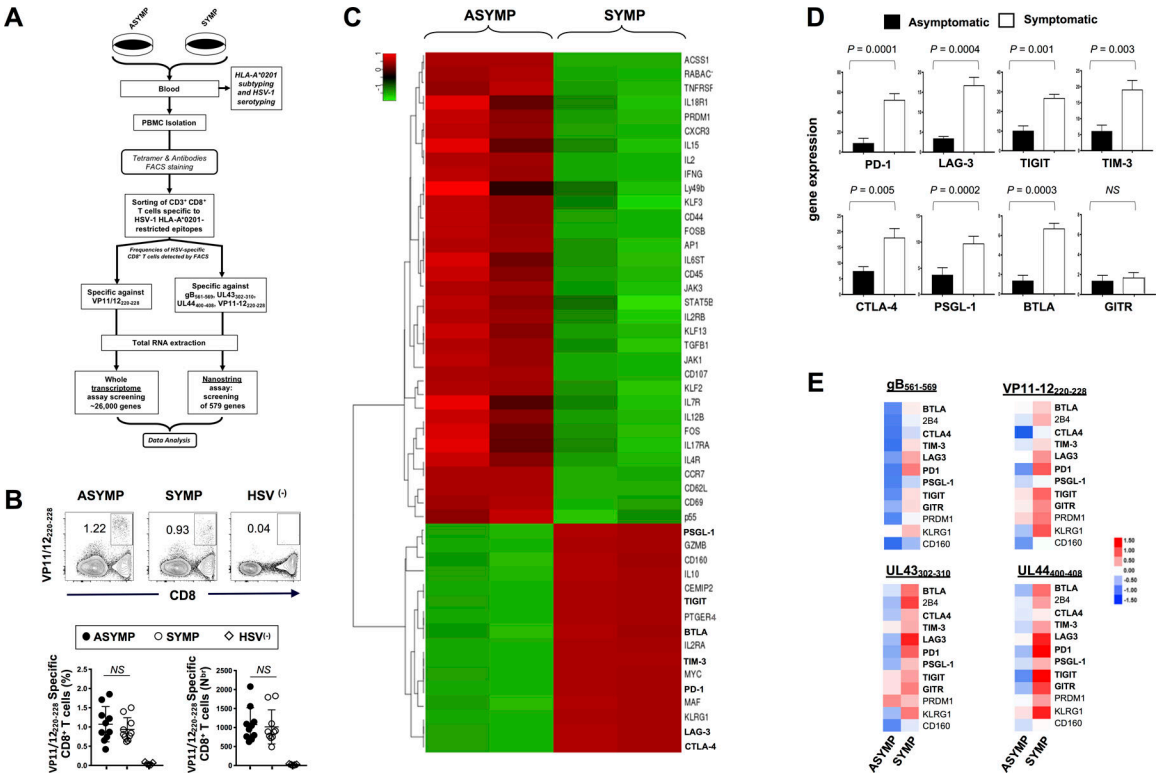

Figure 1: Differential expression of genes for major exhaustion pathways in HSV-specific CD8$^+$ T cells from HSV-1 seropositive symptomatic vs. asymptomatic individuals:

(**A**) Experimental design and validation of differentially expressed genes in CD8$^+$ T cells sharing the same HSV-1 epitope-specificities, from SYMP and ASYMP individuals. CD8$^+$ T cells specific to HLA-A*0201-restricted HSV-1 VP11/12$_{220–228}$ epitope (RLNELLAYV) were sorted from HLA-A*0201-positive SYMP and ASYMP individuals. Total RNA was extracted from each clone of epitope-specific CD8$^+$ T cells, and whole transcriptome analysis was performed using bulk RNA sequencing and NanoString digital barcoding technology to compare the expression levels of 26,000 genes. (**B**) Representative FACS plot of the frequencies of HSV-1 VP11/12$_{220–228}$-specific CD8$^+$ T cells in HSV-1 seropositive SYMP vs. ASYMP individuals and in seronegative healthy individuals (*HSV*$^{(–)}$) (*upper panels*). Average percentages of HSV-1 VP11/12$_{220–228}$-specific CD8$^+$ T cells in 10 SYMP vs. 10 ASYMP individuals (*lower panels*). PBMCs from 5 HSV$^{(–)}$ seronegative individuals were used as control of the tetramer staining (**C**) Bulk RNA sequencing heat map showing differentially expressed immune genes (DEGs) in VP11/12$_{220–228}$ epitope-specific CD8$^+$ T cells from sex- and age-matched HSV-1 seropositive SYMP vs. ASYMP individuals. (**D**) Average expression of eight major exhaustion receptor genes detected through RNA sequencing in VP11/12$_{220–228}$-specific CD8$^+$ T cells from ASYMP and SYMP individuals (**E**) Expression of twelve exhaustion-related genes detected using NanoString technology in CD8$^+$ T cells, that shared the same gB$_{561–567}$, VP11/12$_{220–228}$, UL43$_{302–310}$ and UL44$_{400–408}$ epitopes specificities, sorted from 10 SYMP vs. ASYMP individuals. The indicated *P* values, determined using unpaired *t* test, compared differential gene expression between SYMP and ASYMP individuals.

Author Manuscript Author Manuscript Author Manuscript Author Manuscript

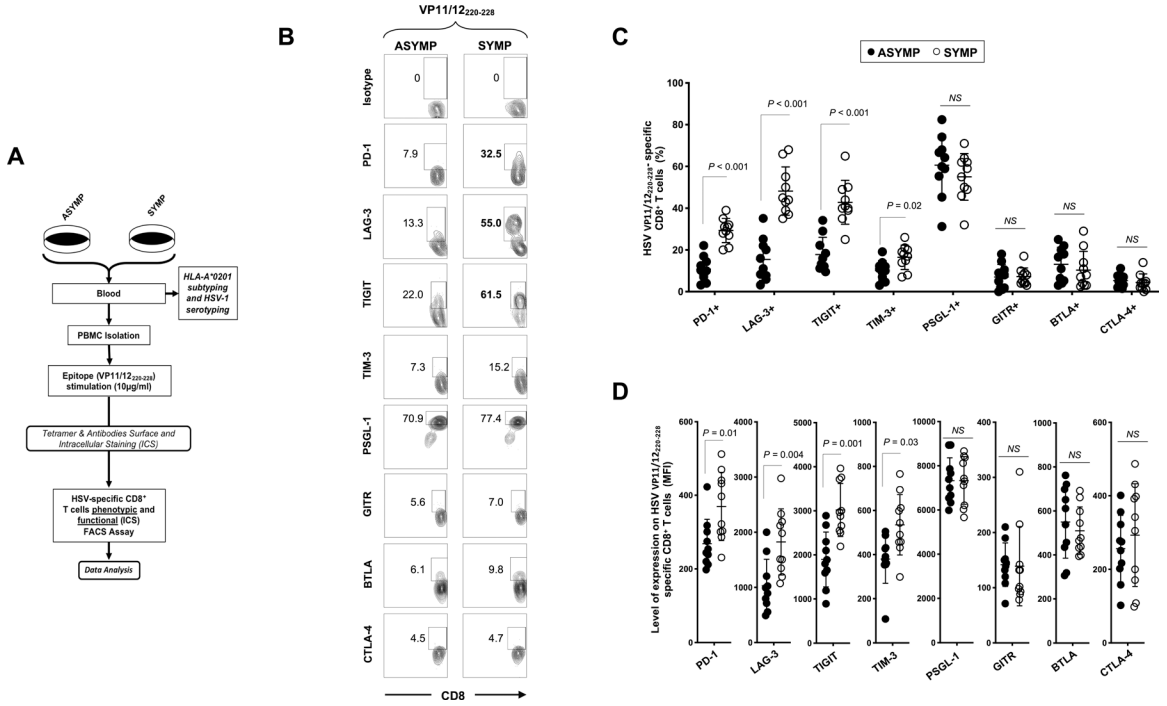

Figure 2: Cell surface expression of exhaustion receptors by HSV VP11/12$_{220–228}$ epitope-specific CD8$^+$ T cells from symptomatic vs. asymptomatic individuals:

(**A**) Experimental design for differentially expressed exhaustion molecules detected by FACS on the surface of CD8$^+$ T cells sharing the same HSV-1 epitope-specificities, from SYMP and ASYMP individuals. PBMCs from 10 SYMP and 10 ASYMP individuals were stained for CD3/CD8, VP11/12$_{220–228}$ tetramer and different exhaustion markers or the isotypic control with the same fluorochrome. The gating strategy is shown in Fig. S1. (**B**) Representative FACS plots and (**C**) average frequencies of HSV-1 VP11/12$_{220–228}$-specific CD8$^+$ T cells expressing PD-1, LAG-3, TIGIT, TIM-3, PSGL-1, GITR, BTLA and CTLA-4 receptors, detected from SYMP vs. ASYMP individuals. (**D**) Levels of expression of the eight exhaustion receptors on HSV-1 VP11/12$_{220–228}$-specific CD8$^+$ T cells from SYMP and ASYMP individuals, depicted as Mean fluorescent Intensity (MFI). Each staining was performed in duplicate. The data are expressed as means +/− the standard deviations (SD). The indicated *P* values, determined using unpaired *t* test, compared expression of exhaustion receptors between SYMP and ASYMP individuals.

Author Manuscript Author Manuscript Author Manuscript Author Manuscript

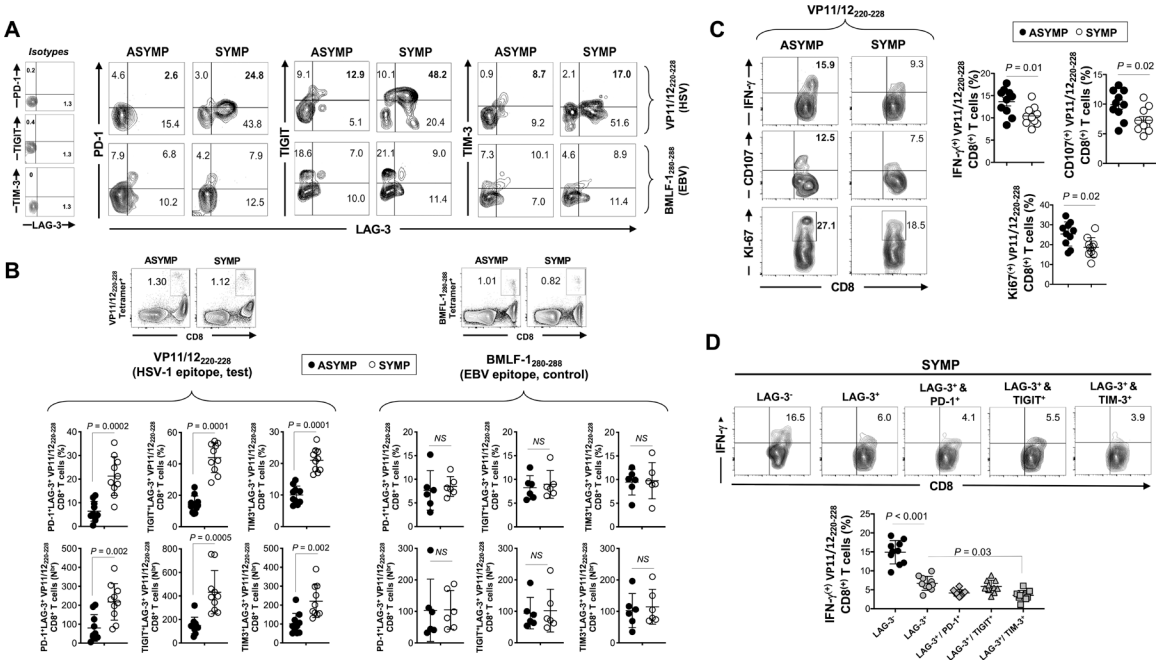

Figure 3: Frequency and function of HSV-1 VP11/12$_{220–228}$ epitope-specific CD8$^+$ T cells, co-expressing LAG-3 with PD-1, TIGIT and TIM-3 receptors, in SYMP vs. ASYMP individuals.

(**A**) Representative FACS plots of the frequencies of HSV-1 VP11/12$_{220–228}$-specific CD8$^+$ T cells (*upper row*) or control EBV BMFL-1$_{280–288}$-specific CD8$^+$ T cells (lower row) co-expressing LAG-3/PD-1, LAG-3/TIGIT and LAG-3/TIM-3 in SYMP and ASYMP individuals. *On the right*: FACS plots representing the isotype controls staining. (**B**) Average percentages (*upper row*) and absolute numbers (*lower row*) of HSV-1 VP11/12$_{220–228}$-specific CD8$^+$ T cells (*left panels*) and control EBV BMFL-1$_{280–288}$-specific CD8$^+$ T cells (*right panels*) co-expressing LAG-3/PD-1, LAG-3/TIGIT and LAG-3/TIM-3 in SYMP and ASYMP individuals. Representative FACS plots of the HSV-1 (VP11/12$_{220–228}$) and EBV (BMFL-1$_{280–288}$) tetramer staining are displayed on the top of each left and right panel, respectively. (**C**) Representative FACS plots (*left panels*) and average (*right panels*) frequencies of functional HSV-1 VP11/12$_{220–228}$-specific CD8$^+$ T cells expressing IFN-γ, CD107$^{a/b}$ and Ki-67 from SYMP vs. ASYMP individuals. (**D**) Representative FACS plots (*top panels*) and average percentages (*lower panels*) of functional HSV-1 VP11/12$_{220–228}$-specific IFN-γ$^+$CD8$^+$ T cells gated on the LAG-3$^–$, LAG-3$^+$, LAG-3$^+$/PD-1$^+$, LAG-3$^+$/TIGIT$^+$ and LAG-3$^+$/TIM-3$^+$ T cell populations. Each staining was performed in duplicate. The indicated *P* values, determined using unpaired *t* test, compared expression of exhaustion receptors between SYMP and ASYMP individuals (B and C) and between cell populations (D).

Author Manuscript Author Manuscript Author Manuscript Author Manuscript

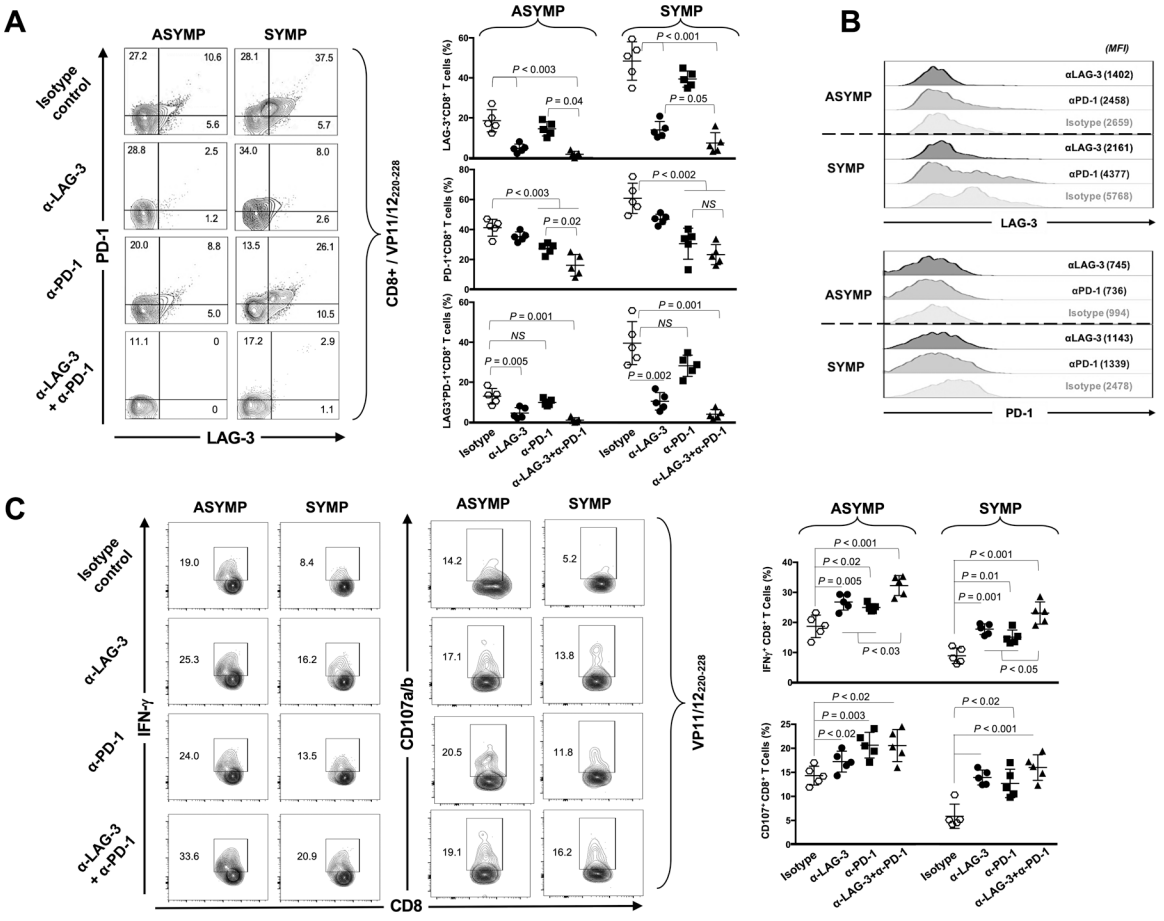

Figure 4: *In vitro* blockade of LAG-3 and/or PD-1 immune checkpoints and reversion of functional exhaustion of HSV-1 VP11/12$_{220–228}$-specific CD8$^+$ T cells from SYMP individuals.

(**A**) Representative FACS plots (*left panels*) and average percentages (*right panels*) of HSV-1 VP11/12$_{220–228}$-specific CD8$^+$ T cells expressing PD-1$^+$, LAG-3$^+$ and LAG-3$^+$/PD-1$^+$ from 5 ASYMP and 5 SYMP individuals, following *in vitro* blockade of the LAG-3 and/or PD-1 immune checkpoints. (**B**) Levels of expression and co-expression of LAG-3 and PD-1 on HSV-1 VP11/12$_{220–228}$-specific CD8$^+$ T cells following *in vitro* blockade of LAG-3 and/or PD-1 immune checkpoints. (**C**) Representative FACS plots (*left panels*) and average percentages (*right panels*) of functional HSV-1 VP11/12$_{220–228}$-specific IFN-γ$^+$CD8$^+$ and CD107$^{a/b+}$CD8$^+$ T cells from 5 ASYMP and 5 SYMP individuals, following *in vitro* blockade of LAG-3 and/or PD-1 immune checkpoints. Each staining was performed in duplicate. The indicated *P* values, determined using unpaired *t* test, compared the frequency and function of CD8$^+$ T cells, following LAG-3 and/or PD-1 blocking mAbs with isotype control mAb.

Author Manuscript Author Manuscript Author Manuscript Author Manuscript

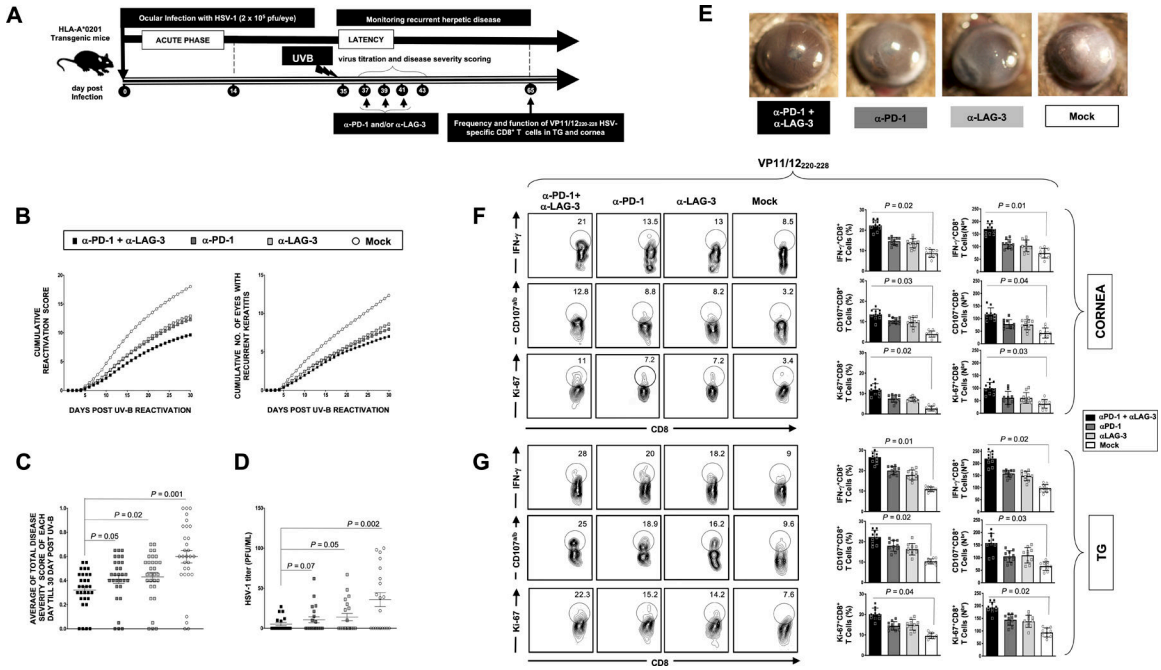

Figure 5: *Effect of in vivo* blockade of PD-1 and/or LAG-3 immune checkpoints on recurrent ocular herpes infection and disease.

(**A**) Schematic representation of HSV-1 ocular infection, α-PD-1 and/or α-LAG-3 blockade treatment, UV-B induced reactivation, virological and immunological analyses in HSV-1 infected HLA-A*0201 Tg mice (*n* = 40; 10 per condition of blockade treatment). (**B**) Cumulative recurrent corneal herpetic lesions (*left panel*) and cumulative number of eyes with recurrent corneal lesions (*left panel*) detected 30 days post UV-B exposure. The severity of corneal herpetic lesions was scored on a scale of 0 to 4. (**C**) Average scores of recurrent corneal disease detected 30 days post UV-B exposure. (**D**) Average titers of the virus shed in the cornea of treated and untreated HSV-1 infected HLA-A*0201 Tg mice. (**E**) Representative images of recurrent corneal herpetic disease taken from treated and untreated HSV-1 infected HLA-A*0201 Tg mice 20 days post UV-B induced reactivation. (**F** and **G**) Representative FACS plots (*left panels*) and average percentages and numbers (*right panels*) of functional HSV-1 VP11/12$_{220–228}$-specific IFN-γ^{+}CD8^{+}, CD107$^{a/b+}$CD8^{+} and Ki67^{+}CD8^{+} T cells detected in the cornea (**F**) and TG (**G**) of treated and untreated HSV-1 latently infected HLA-A*0201 Tg mice. Results are representative of two independent experiments. The indicated *P* values, calculated using the unpaired *t*-test, show statistical significance between mAb treated and untreated control groups.

Author Manuscript Author Manuscript Author Manuscript Author Manuscript

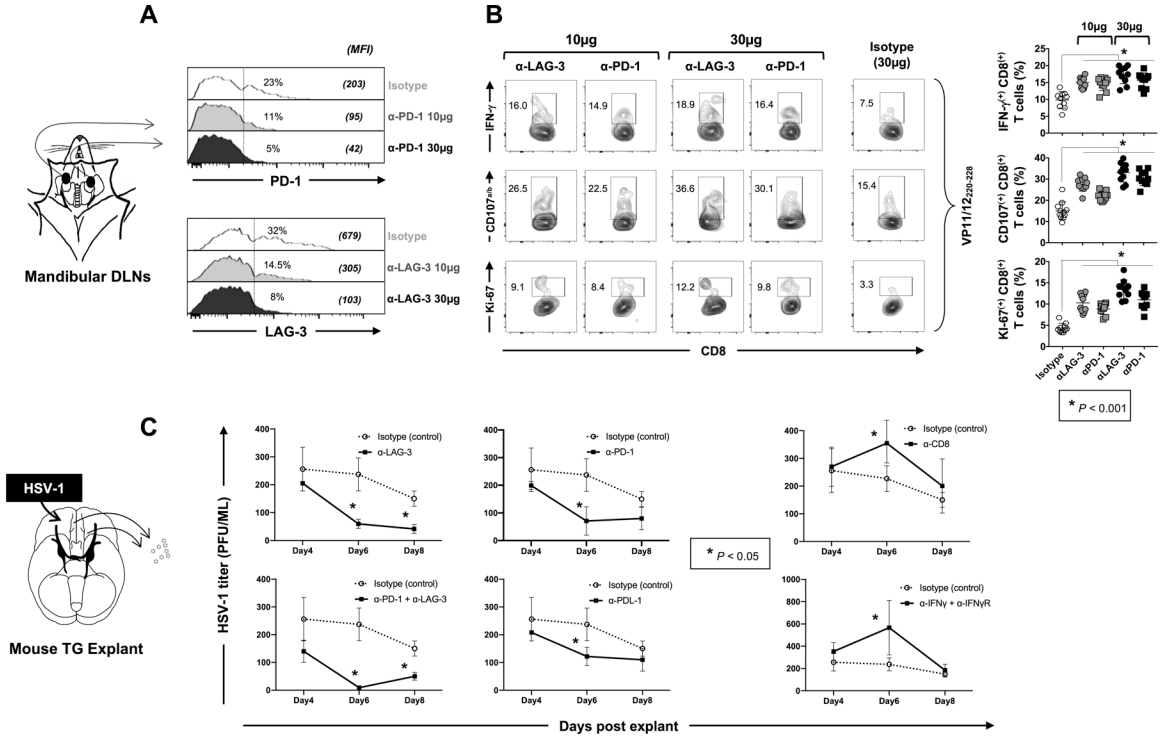

Figure 6: *Effect of ex vivo* blockade of PD-1, LAG-3 and/or TIM-3 immune checkpoints on function of HSV-specific CD8$^+$ T cells and virus reactivation from TG explants of HSV-1 infected HLA-A*0201 transgenic mice.

HLA-A*0201 Tg mice (n =10 per group of blockade treatment) were ocularly infected with HSV-1 (2.5×10^5 pfu per eye, strain McKrae). Fourteen days post-infection CD8$^+$ T cells derived from submandibular lymph nodes were stimulated for 12 hours with 10 μg/mL of VP11/12$_{220–228}$ peptide ("RLNELLAYV"). Blocking α-LAG-3 and/or α-PD-1 mAbs were added in the culture for two additional days (at either 10 μg/mL or 30 μg/mL). (**A**) Representative histograms display the levels of expression of LAG-3 or PD-1 depicted by the MFI on HSV-1 VP11/12$_{220–228}$-specific CD8$^+$ T cells from HSV-1 infected HLA-A*0201 Tg mice following blockade of LAG-3 or PD-1 immune checkpoints. (**B**) Representative FACS plots of the percentages of functional HSV-1 VP11/12$_{220–228}$-specific IFN-γ$^+$CD8$^+$, CD107$^{a/b+}$CD8$^+$ and Ki-67$^+$CD8$^+$ T cells following *in vitro* blockade of LAG-3 or PD-1 immune checkpoints. (**C**) Fourteen days post-infection, cell suspensions from TG explants were incubated in duplicates with 100 μg/mL of α-LAG-3 and/or α-PD-1 blocking mAbs or isotype control mAb. Graphs show the level of reactivated virus (expressed in PFU/mL) detected in the supernatant of TG explants on 4, 6- and 8-days post-incubation. The data are expressed as means +/− the standard deviations (SD). The indicated *P*-values, calculated using the unpaired *t* test, show the statistical significances between the control (Isotype) and the different blocking conditions. The results showed here are representative of two independent experiments.

Author Manuscript

Author Manuscript

Author Manuscript

Author Manuscript

Table 1

Cohorts of HLA-A*02:01 positive, HSV seropositive Symptomatic and Asymptomatic individuals enrolled in the study

Subject-level Characteristic	All Subjects (n = 30)	ASYMP (n = 15)	SYMP (n = 15)	HSV $^{(-)}$ (n = 5)
Gender [no. (%)]:				
Female	15 (50%)	8 (53%)	7 (47%)	2 (40%)
Male	15 (50%)	7 (47%)	8 (53%)	3 (60%)
Race [no. (%)]:				
Caucasian	21 (70%)	11 (73%)	10 (67%)	4 (80%)
Non-Caucasian	9 (35%)	4 (27%)	5 (33%)	1 (20%)
Age [median (range) yr.]:	40 (23–55)	42 (26–55)	39 (23–55)	36 (28–45)
HSV status [no. (%)]:				
HSV-1-seropositive	30 (100 %)	15 (100%)	15 (100%)	0
HSV-2-seropositive	0 (0%)	0	0	0
HSV-1- & 2-seropositive	0 (0%)	0	0	0
HSV-seronegative	0 (0%)	0	0	5 (100%)
EBV-seropositive	12 (40%)	6 (40%)	6 (40%)	N/A
HLA [no. (%)]				
HLA-A*02:01-positive	30 (100%)	15	15	5
HLA-A*02:01-negative	0 (0%)	0	0	0
Herpes Disease Status [no. (%)]				
Asymptomatic (ASYMP)	15 (50%)	N/A	N/A	N/A
Symptomatic (SYMP)	15 (50%)			